Positron annihilation in liquids and in solutions containing electron acceptors and charge-transfer complexes

Jansen, P.

Publication date:
1976

Document Version
Publisher's PDF, also known as Version of record

Risø Report No. 333

Risø Report No. 333

Research Establishment Risø

Positron Annihilation in Liquids and in Solutions Containing Electron Acceptors and Charge-Transfer Complexes

by Peter Jansen

May 1976

Sales distributors: Jul. Gjellerup, 87, Sølvgade, DK-1307 Copenhagen K, Denmark

Available on exchange from: Risø Library, Research Establishment Risø, DK-4000 Roskilde, Denmark

May 1976 Risø Report No. 333

Positron Annihilation in Liquids and in Solutions Containing Electron Acceptors and Charge-Transfer Complexes

by

Peter Jansen

Research Establishment Risø
Chemistry Department

Abstract

Positron lifetime measurements and angular correlation measurements were performed in several organic liquids. The results strongly indicate that positronium is contained in a "bubble" in the liquids. The radius of the bubble can be estimated by using the broadness of the narrow component in the angular correlation distribution, and by using the surface tension of the liquids. Both methods give bubble radii from 4-7 Å in the solvents investigated. The bubble influences the reaction mechanism between Ps and weak electron acceptors in such a way that the presence of the bubble decreases the reactivity of Ps. Positron lifetime measurements were also performed on a series of mixtures of organic liquids and on electron acceptors and charge-transfer complexes in solution. The results were in agreement with the spur reaction model of Ps formation, which, for the binary mixtures, explains the influence on Ps formation of proton spur reactions, in other cases of the solvation of spur electrons and positrons, and finally of electron trapping on CS_2 combined with high electron mobility in pure CS_2. The electron trapping ability of CS_2 is expected to depend on the V_o of the solvent in which the CS_2 is dissolved. This dependence was observed. The electron acceptors give rise both to Ps inhibition (with two

possible exceptions) and quenching, but when an acceptor takes part in a charge-transfer complex, the inhibition intensifies and the quenching almost vanishes. The decreased quenching was used to determind complexity constants that were in reasonable agreement with constants obtained from optical data. PV technique was also introduced to determine gas phase complexity constants. By use of the spur reaction model, the Ps yields were correlated to the gas phase reaction between electron acceptors and free electrons, as well as to pulse radiolysis data.

ISBN 87-550-0401-6

CONTENTS

1. INTRODUCTION

This report describes the use of positron annihilation technique (PAT) as a tool to obtain information about different chemical reactions and systems. The study of binary mixtures of organic solvents and solutions containing electron acceptors and charge-transfer complexes is chiefly described. The aim of the work is to clarify the parameters determining the amount of positronium (Ps) formed when energetic positrons are injected into a solvent and the reactions of the Ps formed.

This report is submitted to Copenhagen University in partial fulfilment of the requirements for the degree of lic. scient. (Ph. D.). With some minor changes major parts have already been published in two articles[1,2].

Interest in low energy positrons and Ps started to develop in the early 1950's. Since then one European and three international PAT conferences have taken place. A fourth international PAT conference will be held in August 1976.

To date, roughly 1000 articles on PAT have been published. Several of them being review articles[3-9]. The annual number of articles dealing with the PAT field is currently (1975) approx. 200. The work described is done in more than 15 different countries. Nearly half the articles concern the study of metals, where topics such as Fermi surfaces, and defects in metals have been investigated using PAT. Especially for studies of defects in metals, PAT can give important information unobtainable by other methods. In chemistry, PAT was earlier mainly used for the study of Ps reactions; but since the proposal of the spur reaction model[10] PAT has also been used to study the reactions of "excess" electrons within the ps region. Thus PAT gives information of importance to radiation chemistry.

In addition, subjects such as ionic crystals, molecular crystals, positrons and Ps in gases and Ps states, have been investigated by use of PAT.

2. THE POSITRON AND POSITRONIUM

The positron (e^+) is an elementary particle with a rest mass equal to the rest mass of an electron and a charge equal to that of a proton.

The positron was first experimentally verified by Anderson in 1932[11,12]. On a photographic plate showing the tracks of cosmic radiation in a magnetic field, he ascribed a track to a positive particle - of which the mass was much closer to that of an electron than to that of a proton. Already in 1930 Dirac, in his "hole" theory, had put forward possible existence of a positive electron[13].

When epithermal positrons are injected into a organic solvent they may form positronium, (Ps). Ps is a bound state between a positron and an electron, in many respects similar to the hydrogen atom. The ground-state binding energy of Ps is half that of H[3]. The radius in the relative movement of the positron and the electron is two Bohr radii, giving an effective diameter of Ps equal to that of H.

$$E_{Ps} = 6.8 \text{ eV} \quad (2.1)$$

$$D_{Ps} = 1.06 \text{ Å} \quad (2.2)$$

This is due to the reduced mass of Ps, which is half that of H. Similar to the electron, the positron has a spin equal to 1/2 h.

Ps exists in two different spin states. Singlet - (1 Ps) or para - Ps(p-Ps), where the spins of the electron and the positron are opposite to each other, and triplet - (3 Ps) or ortho - (o-Ps), where the spins of the positron and electron are parallel to each other. In the absence of a magnetic field, o-Ps can exist in three degenerated states. p-Ps can only exist in one state.

A positron can annihilate with an electron. This means that they are both converted into Y-irradiation. In vacuum p-Ps will annihilate through 2Y annihilation with a characteristic lifetime of 0.125 ns. (1 ns = 10^{-9} s). Since Y-rays are spin 1 particles it is necessary to use two Y-rays with opposite spin in order to obtain spin conservation.

PROPERTIES OF POSITRONIUM (Ps)

TYPE	STATE	SPIN	QUANTUM NO.	DECAY MODE	LIFETIME	FRACTION
PARA ^{1}Ps	SINGLET	↑↓	I = 0 m = 0	2Y	125 ps	25%
ORTHO ^{3}Ps	TRIPLET	↑↑	I = 1 m = 0, ± 1	3Y	137ns	75%
	PICK - OFF			2Y	~1ns	

Fig. 1. Properties of positronium (Ps).

Due to energy and momentum conservation during the annihilation process the energy of each of the two Y-rays will be equal to the rest energy of an electron if the p-Ps has zero momentum at the time of annihilation.

$$E(\gamma) = m_e c^2 = 0.511 \text{ MeV} \tag{2.3}$$

where m_e is the rest mass of the electron and c the velocity of light. Due to momentum conservation, the two Y-rays will be emitted in almost opposite directions. The deviation θ, from the angle π between the two rays is for small θ.

$$\theta \simeq \arcsin\left(\frac{p}{m_e c}\right) \tag{2.4}$$

where p is the total momentum of the annihilating positron - electron pair perpendicular to the direction of Y-ray emission. θ is normally a few milliradians so

$$\theta \simeq \frac{p}{m_e c} \ . \tag{2.5}$$

As a result of spin conservation, o-Ps can only annihilate through the emission of an odd number of Y-rays. In vacuum, at least three Y-rays are necessary in order to obtain spin and momentum conservation. In vacuum o-Ps annihilates through 3Y annihilation with a characteristic lifetime of 137 ns.

In condensed matter the positron in o-Ps will normally not annihilate with its own electron. The positron will instead annihilate through 2Y annihilation with an electron in one of the outer orbitals of the solvent molecules and the electron will have a spin opposite that of the positron. This type of annihilation is called pick-off annihilation. Naturally, pick-off annihilation reduces the lifetime of o-Ps in liquids. A typical o-Ps lifetime in organic liquids is 1-5 ns.

The free positrons in the liquid, e.g. positrons which have not formed Ps, will also annihilate through 2Y annihilation with an electron in a molecular orbital. This electron will have a spin opposite that of the positron. A characteristic lifetime for free positrons in organic liquids is 0.3-0.5 ns.

In order to obtain information about the fate of the positrons, different measuring systems have been developed. The most commonly used are: positron lifetime measurements, angular correlation measurements and finally Doppler-broadening. Each of these systems are briefly sketched in

this section, and the next section gives a more detailed description of the lifetime system and the angular correlation system.

^{22}Na is used as positron source. The decay scheme of ^{22}Na is shown on fig. 2.

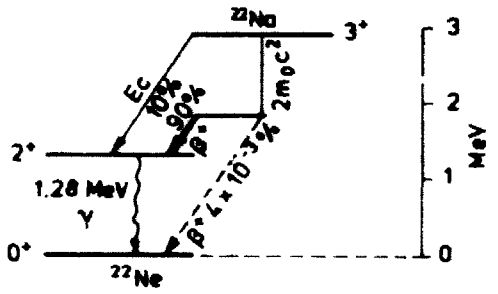

Fig. 2. Decay scheme of ^{22}Na.

The half-life of ^{22}Na is 2.6 years. The positrons are emitted from ^{22}Na with energies ranging from zero and up to 0.54 MeV. A γ-ray at 1.28 MeV is emitted almost simultaneously with the ^{22}Na emission of a positron. This 1.28 MeV γ-ray announces the formation of a positron and is used as starting signal in positron lifetime measurements. The 0.511 MeV signal announcing the annihilation of the positron is then used as a stopping signal in the lifetime system. The time between the two signals is measured, and a positron lifetime spectrum is the number of positrons existing during this particular time as a function of time. Such a spectrum is normally composed of a sum of decaying exponentials. For this reason it is often shown as the logarithm of the number of positrons versus the time.

In angular correlation measurements the angle θ between the two 0.511 MeV photons is measured. This system consists of one fixed and one moveable detector. The number of coincident signals from the two detectors is then measured as a function of the angle θ. In the free particle approximation, θ is roughly proportional to the z-component of the momentum of the annihilating positron - electron pair (see fig. 4). In the independent particle approximation the momentum distribution can be calculated as the Fourier-transform of the product of the positron, and the electron wave function. For Ps in vacuum the momentum distribution can be calculated as the Fourier-transform of the Ps centre of mass wave function. An example of such a calculation is given in section 5.

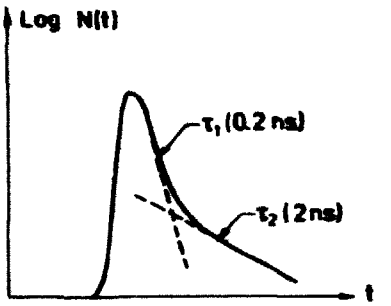

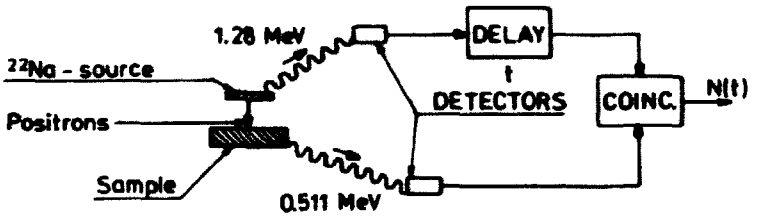

POSITRON LIFETIME TECHNIQUE

Fig. 3. A two-component positron lifetime spectrum and the principle in a set-up for positron lifetime measurements.

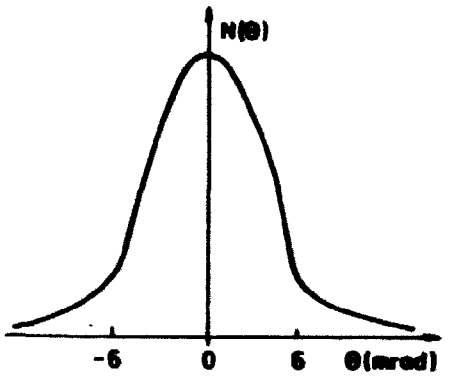

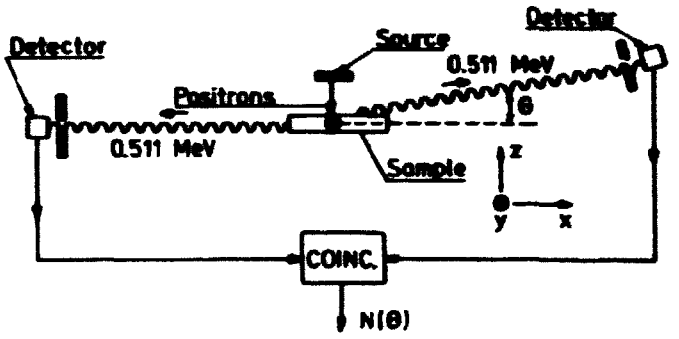

ANGULAR CORRELATION TECHNIQUE

Fig. 4. A typical angular correlation spectrum for a metal, and the principle in a set-up for angular correlation measurements.

In the case of p-Ps, where the total momentum is proportional to the centre of mass velocity, we get a rather narrow angular correlation function for thermal p-Ps. For pick-off annihilation, the positron -electron momentum will be roughly proportional to the velocity of the electron in the molecular orbit. Such a velocity can correspond to a kinetic energy of several eV and, compared to the p-Ps will give rise to a broad angular correlation function. For the same reason, the free positrons in the liquid also cause a broad angular correlation function.

In the Doppler-broadening experiment the energy of the annihilation quanta is measured. Here again the quanta have to carry the total energy and momentum of the annihilating pair. It appears that the major part of the deviation from the rest mass energy 0.511 MeV of the γ-quanta originates from the momentum conservation and not from the energy conservation[14]. The γ-spectrum of the annihilation quanta will be broadened due to the momentum of the positron-electron pair in the direction of the γ-ray propagation. Consequently, the information obtained from Doppler-broadening experiments is very similar to the information obtained from angular correlation experiments. One of the advantages of Doppler broadening is that the counting rate is very high. This means that there is a short measuring time for Doppler-broadening experiments compared to angular correlation experiments. A disadvantage of Doppler broadening is the rather poor resolution obtainable compared to the resolution in angular correlation measurements.

A more detailed description of the positron annihilation process and the calculation of the o- and p-Ps lifetime is given in books on quantum electrodynamics[15].

3. APPARATUS

A diagram showing a typical fast-slow coincidence system for positron lifetime measurements is shown in fig. 5. The system consists of two detectors a fast circuit (on the figure the outer) and a slow circuit (the inner circuit on the figure). The two detectors are identical and each consists of a cylindrical 1.5" x 1.5" scintillator-doped plastic "crystal" (NE 111 or Naton 136). Each plastic scintillator is mounted on a fast photomultiplier tube (PM).

The fast circuit is responsible for the time measurement and the slow system ensures that only signals from the time to amplitude converter (TAC) that originate from a 1.28 MeV photon followed by a 0.511 MeV photon are allowed into the multi-channel analyser (MCA).

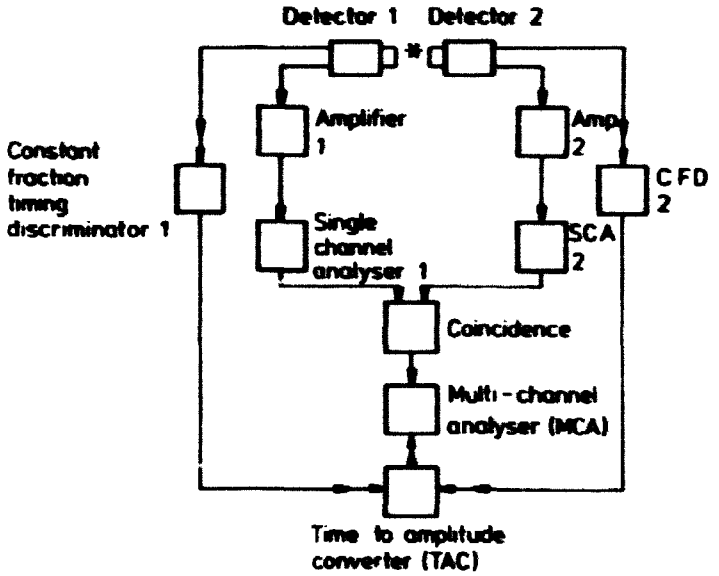

Fig. 5. A diagram of typical equipment for positron lifetime measurements.

When, for example, a 1.28 MeV photon is absorbed by the scintillator crystal, the crystal will emit light which can result in a signal from the PM tube. The signals from the PM tube are of different magnitude and can often have a rise time of more than 1 nsec and a full width half maximum (FWHM) of 2-3 nsec. These signals are very broad and slow, considering that they are to be used to measure time differences as low as 100-200 ps. Thus, a special technique was developed in order to obtain a reliable method to measure the peak position of such a pulse. This technique is applied in the so-called constant fraction discriminators (CFD). Assume that the pulses to the discriminators can be approximated with a Gaussian

$$P = -A \exp(-at^2) \qquad (3.1)$$

where A, a are positive constants and t the time. When this pulse enters the CFD it is inversed and delayed and then added to the attenuated input pulse. The resulting pulse is

$$R_P = -A(k \exp(-at^2) - \exp(-a(t-t_o)^2)) \qquad (3.2)$$

where t_o is the delay time and $o < k < 1$ is determined by the attenuation of the original pulse. When P_R changes from negative to positive values, it opens a gate and a standard pulse leaves the CFD. From (3.2) it can be seen that the zero value of P_R is independent of the amplitude A. This means that although the leading edge of two pulses with different amplitudes, dispatched with a time difference T, will arrive at the CFD with a time difference different from T, the two standard pulses leaving the CFD will again have a time difference T. Thus the use of a CFD instead of a leading edge discriminator improves the time resolution of the system, especially if the pulses are of rather different amplitudes. Normally the pulses are asymmetrical so the use of a single Gaussian is a poor approximation. But as long as t_o is less than the rise time of the pulses, it is only important that the front edge of the pulses can be approximated with a Gaussian.

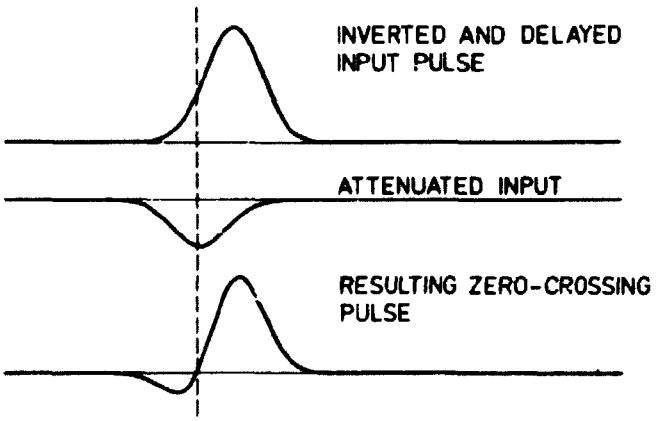

Fig. 6. Gaussian approximation of the inverted and delayed input pulse, the attenuated input pulse and the resulting zero-crossing pulse used in the constant fraction discriminator.

Apart from being divided into a fast and a slow circuit, the system is also divided into a starting system (e.g. system 1 on fig. 5) and a stopping system (e.g. system 2 on fig. 5). A typical lifetime measurement can take place as follows.

A 1.28 MeV γ-ray is absorbed in detector 1 and a pulse is dispatched from PM1. In the fast circuit, this pulse initiates a pulse from CFD1 and the TAC will "begin to measure the time". In the slow circuit, the pulse passes an amplifier and from there enters single channel analyser 1 (SCA),

which dispatches a pulse if the incoming pulse is of a magnitude corresponding to a 1.28 MeV photon. The 0.511 MeV annihilation photon initiates a pulse from CFD2. When this pulse reaches the TAC, the TAC dispatches a pulse with an amplitude proportional to the time difference between the signal from CFD1 and CFD2. The pulse from the TAC will only be allowed into the MCA if the MCA simultaneously receives a signal from the coincidence "box". This "box" only dispatches a signal if, within a preset time interval, it receives a signal from SCA1 (from a 1.28 MeV photon) and a signal from SCA2 (from a 0.511 MeV photon).

If, for example, two independent 0.511 MeV photons cause signals in PM1 and PM2, the signal from the TAC is not stored in the MCA, since SCA1 rejects the signal for energy reasons and consequently the coincidence "box" does not open the MCA.

The MCA simply registers the number of the positrons which have existed during that particular time versus the time. Cobolt-60 emits two γ-rays, practically simultaneously with energies which are able to pass SCA1 and SCA2. The signals from ^{60}Co should, in principle, all enter the same channel in the MCA corresponding to time zero. In practice, it turns out that the ^{60}Co spectrum occupies several channels in the MCA. This is due to the finite time resolution of the apparatus. This finite time resolution of the apparatus causes a smearing out of the lifetime spectra and plays a very important role in the data analyses.

In order to make a proper analysis of the lifetime spectra it is convenient to have a mathematical approximation to the time resolution, or prompt curve. Normally the prompt curve is fitted with a sum of up to three co- or off-centered Gaussians. A typical FWHM of the prompt curves used was 400 ps.

The set-up used in the angular correlation measurements is sketched on the diagram in fig. 4. The detector at the left is fixed and the detector at the right is movable. Each detector consists of a horizontally mounted Tl-doped NaI crystal connected to two PM tubes. Each detector covered a solid angle of 0.96 mrad in the z direction and 178 mrad in the y direction. Two energy-selecting SCAs should be inserted between the PM tubes and the coincidence box in fig. 4. After passing the SCAs, the signals enter a coincidence "box". Again the box emits a signal if the signals from the SCAs arrive within a preset time interval. The coincidence box ensures that the two photons originate from the same event.

The angular correlation spectrum is the number of coincidences as a function of the angle between the sample and the two detectors.

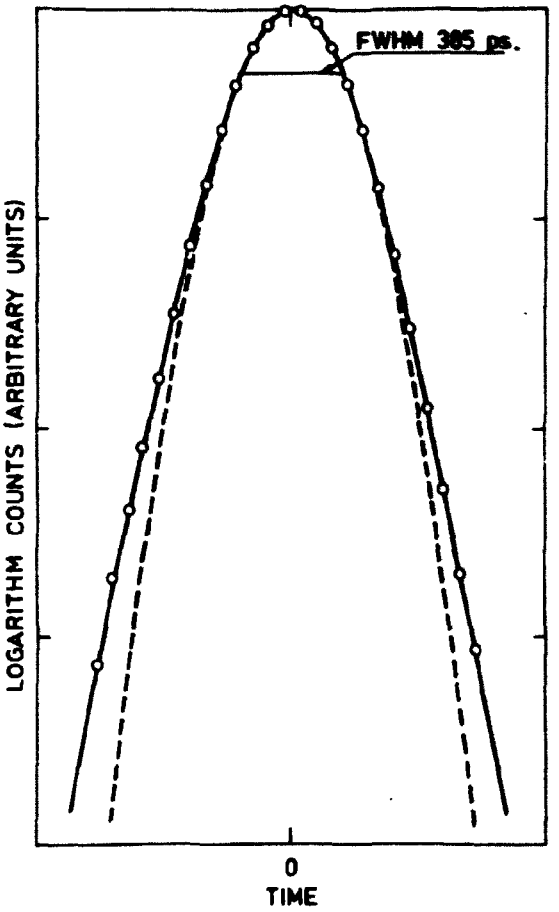

Fig. 7. ^{60}Co prompt(P-)curve. The dashed curve is a single Gaussian approximation having the same FWHM (385 psec) as the experimentally obtained P-curve. The fully drawn curve is a two-Gaussian curve composed of one Gaussian having a FWHM on 370 ps and a relative intensity of 80%, and a Gaussian with a FWHM on 522 ps and an intensity of 20%. The latter curve is off-centered 15 ps to the left of the first curve.

A more detailed description of the positron lifetime set-up is given in ref. 16. A quantum mechanical calculation of the two γ angular correlation functions and the correspondance between these functions and the measured angular correlation spectrum is given in ref. 17.

4. PRINCIPLES OF DATA ANALYSIS

All the recorded and presented lifetime spectra were analysed using the program POSITRONFIT[18,19].

More detailed information about the program is given in the original references[16,18,19].

If the positrons only existed in one state, the positron lifetime spectrum could be described by a single decay exponential

$$N(t) = A \exp(-\lambda t), \tag{4.1}$$

where A is a constant, λ the annihilation rate, and t the time. N(t) is the number of positrons having existed during the time t. Normally the positron can be in j different states (e.g. p-Ps, o-Ps, free e^+) and the lifetime spectra will then be composed of a sum of j decay exponentials.

$$N(t) = \sum_j A_j \exp(-\lambda_j t). \tag{4.2}$$

Here the intensity of the j component I_j (in %) will be given by:

$$I_j = \frac{\frac{A_j}{\lambda_j} \times 100}{\sum_j \frac{A_j}{\lambda_j}}. \tag{4.3}$$

Fig. 8 illustrates how $\tau_j = \lambda_j^{-1}$ and I_j can be found by graphical methods from the lifetime spectra.

The prompt curve can be described as a sum of Gaussians:

$$R(t) = \sum_p c_p G_p(t), \tag{4.4}$$

where

$$G_p(t) = (\sigma_p \sqrt{\pi})^{-1} \exp(-((t-T_o - \Delta t_p)/\sigma_p)^2) \tag{4.5}$$

$$\sum_p c_p = 1 \tag{4.6}$$

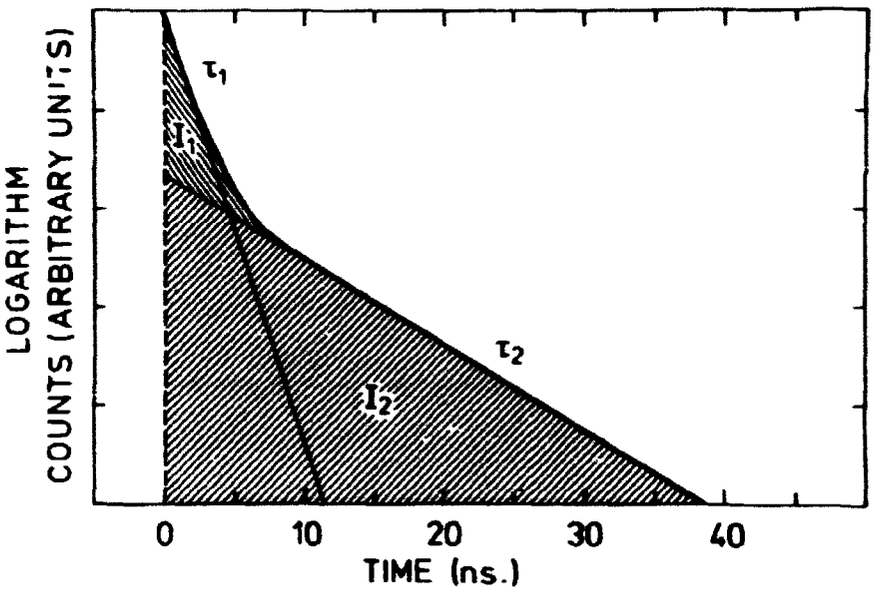

Fig. 8. Synthetic lifetime spectrum composed of two lifetimes on 5 and 1 ns having relative intensities of 10% and 90%, respectively. The lifetimes τ_1 and τ_2 can be obtained from the slope of the two fully drawn lines. The absolute intensities associated with each lifetime is proportional to hatched areas I_1 and I_2

and σ is related to the FWHM

$$\sigma_p = \frac{FWHM_p}{2\sqrt{\ln 2}} \qquad (4.7)$$

T_o corresponds to a reference channel number (time = 0) and Δt is the displacement of the p'th component from T_o.

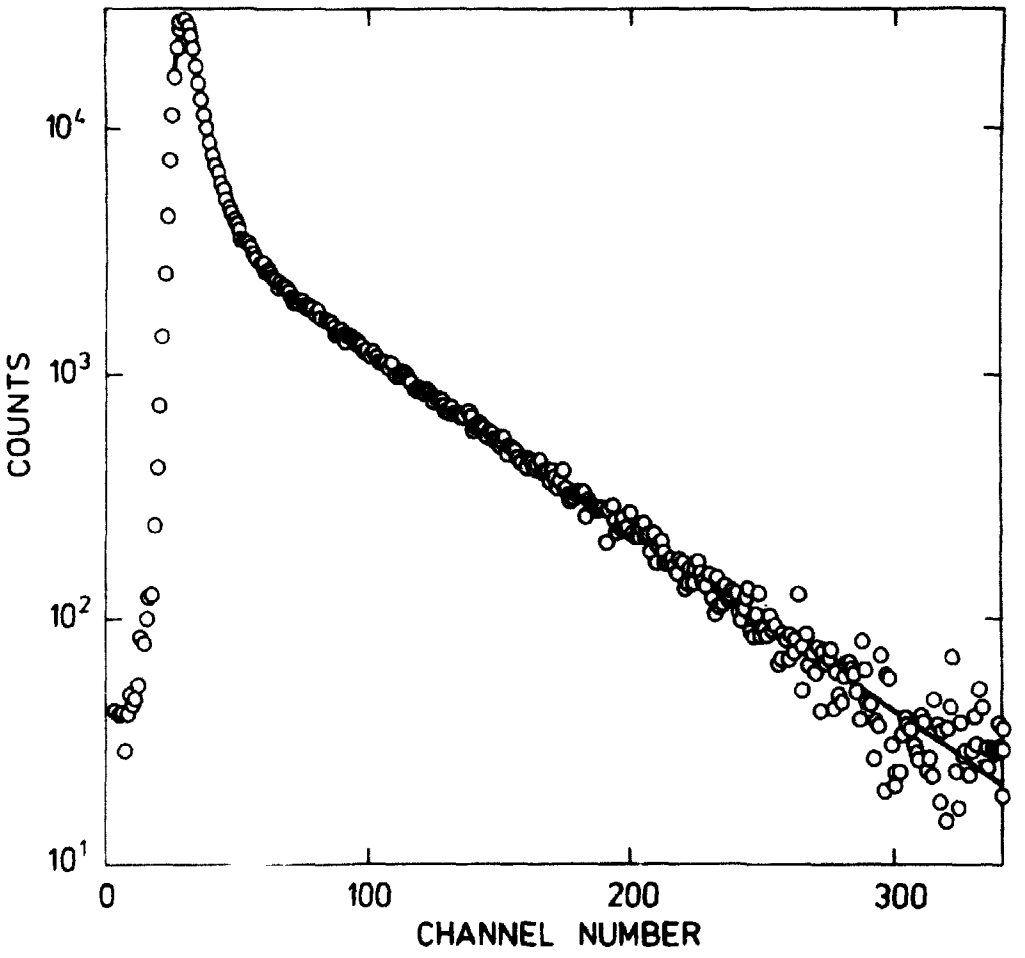

Fig. 9. The lifetime spectrum of 40 vol. % CS_2 in TMS. The fitted curve, which can be seen on the figure in positions where it is not covered by the experimental points, is composed of three decaying exponentials. The time zero corresponds to channel 25.5, the time per channel is 60.2 ps. The curve can be represented by three lifetimes of 0.188 ns, 0.469 ns, and 3.559 ns with relative intensities of 25.83%, 26.16% and 48.01%, respectively.

Theoretically the measured spectrum F(t) will be (4.2) folded with the resolution function (4.5)

$$F(t) = \int_0^\infty R(t-t') \left(\sum_j A_j \exp(-\lambda_j t') \right) dt' + B , \qquad (4.8)$$

where B is the background. This integral F(t) can be evaluated and expressed in analytical functions.

In the analysis of an ordinary lifetime spectrum the prompt curve, with the exception of T_o, is given as input parameter. The program then fits the given spectrum with F(t) having T_o and λ_j's as nonlinear fitting parameters and B and A_j as linear fitting parameters. A typical spectrum is represented by 400 numbers and will be analyzed for three lifetimes and three intensities. Eight parameters will be extracted from such a spectrum. The output from the computer also gives the variance of the fit, the statistical uncertainties on each parameter, plus a matrix of total correlation.

Normally the positron source (^{22}NaCl) is enclosed between two thin Ni, capton or mylar foils. This means that a fraction of the positrons annihilate in the foils surrounding the source. The spectrum of the positrons annihilating in the foils and the fraction of the total number of positrons annihilating in the foils can be determined by different methods.

Normally the lifetime spectrum of the positrons annihilating in the source is calculated and subtracted from the measured lifetime spectra before final analysis of the spectrum.

POSITRONFIT is a versatile program and many kinds of constraints can be imposed on the fitting parameters. All τ's, I's, T_o and the background can be fixed independent of the other parameters. Linear combinations of the intensities may also be fixed to be zero. It is, for example, possible to fix the shape of the lifetime spectrum of a given compound and then see how much of this spectrum there is in the measured spectrum.

The data analyses used for the presented spectra are given in section 6.

The angular correlation curves were fitted by using the program PAACFIT[20]. This program fits the measured spectrum with a sum of Gaussians:

$$R(\theta) = \sum_p A_p \exp(-((\theta - \theta_o)/\sigma_p)^2) . \qquad (4.9)$$

In liquids the theoretical curve will be symmetrical around θ_o. The program can fit the measured curve by use of the A_p's, σ_p's and θ_o. Also this program gives a statistical analysis of fitted parameters. Constraints on the individual parameters, as well as linear combinations of the A's, can be imposed before analysis of a measured spectrum.

Again it is possible to see how much of a given curve is contained in a presented curve.

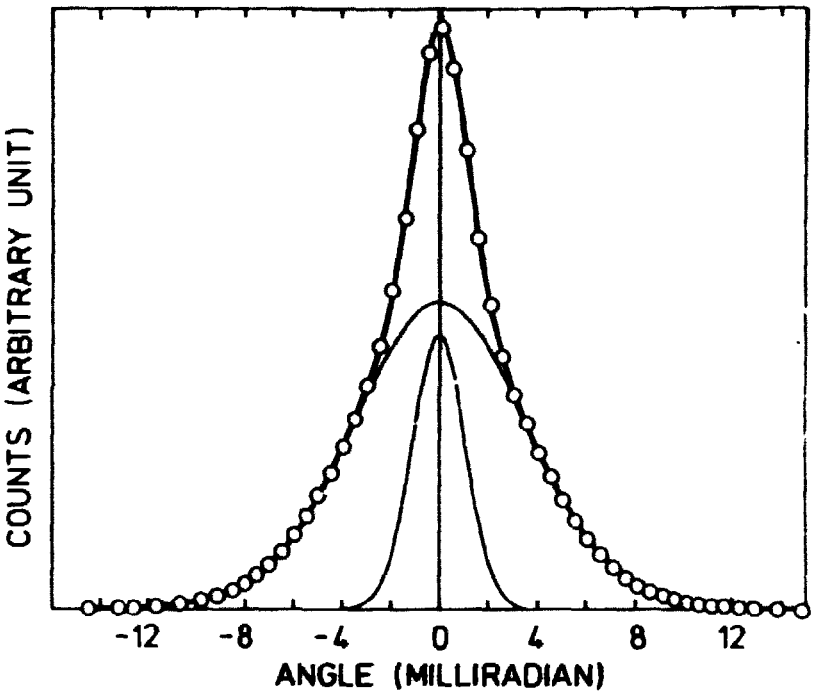

Fig. 10. The angular correlation curve of TMS. The curve drawn with a broad line is composed of three Gaussians having FWHM of 2.53 mrad, 8.11 mrad and 14.93 mrad with relative intensities of 21.17%, 72.89% and 5.94%, respectively. The broad curve drawn with a thin line represents the sum of the two broadest components in the fitting curve. The narrow curve drawn with a thin line represents the narrow component of the fitting curve. This narrow curve is believed roughly to represent the p-Ps momentum distribution.

5. MODELS AND FORMULAS

When epithermal positrons are injected into an organic solvent they can undergo different chemical reactions. Some of the positrons can form o-Ps. The o-Ps 3-Y annihilation rate is λ_t. The o-Ps can also participate in chemical reactions before annihilation. The most relevant reaction is believed to be the following.

In the presence of oxidezers (0x) the o-Ps can be oxidized.

$$Ps + Ox \rightarrow e^{+} + Ox^{-}. \qquad (5.1)$$

The oxidizing rate λ_o can normally be written as

$$\lambda_o = k\,[Ox]\,, \qquad (5.2)$$

where k is the oxidizing rate constant dependent on Ox, the solvent and the temperature. [Ox] is the oxidizer concentration.

Similar to the positrons which have not formed Ps, the free positrons produced by the oxidation will annihilate with a characteristic annihilation rate λ_f.

The o-Ps can also form bound states or complexes with different molecules, e.g. electron acceptors (A)

$$Ps + A \rightarrow PsA\,. \qquad (5.3)$$

The complex formation rate λ_c is

$$\lambda_c = k'\,[A]\,, \qquad (5.4)$$

where k' is a rate constant dependent on A, solvent and temperature.

Another process that o-Ps can undergo is conversion. The o-Ps can be converted into p-Ps. This process normally occurs through interaction with a free radical R.

$$o\text{-}Ps + R \rightarrow p\text{-}Ps + R\,. \qquad (5.5)$$

The conversion rate γ can be written

$$\gamma = k''\,[R]\,. \qquad (5.6)$$

Again k'' is dependent on R, solvent and temperature.

The o-Ps that has not participated in the processes mentioned above will normally annihilate through pick-off annihilation

$$o\text{-}Ps + M \rightarrow e^{-} + M^{+} + 2\gamma \qquad (5.7)$$

where M is a molecule. The pick-off annihilation rate is λ_p.

Some of the positrons injected into a medium can form p-Ps. It is believed that the p-Ps formation probability is 1/3 of the o-Ps formation probability. The Ps formation probability is believed to be independent of

the state into which the Ps converts, and in the absence of a magnetic field there are three degenerated o-Ps states and one p-Ps state. This explains the factor 1/3 for the p-Ps formation probability. The energy difference between o-Ps and p-Ps is $8.4 \cdot 10^{-4}$ eV [3], so in practice, for energy reasons, none of the four different states should be preferred in favour of the others. p-Ps can undergo the same chemical reactions as o-Ps and it is believed that the rates for oxidizing λ_o, complex formation λ_c, and pick-off annihilation λ_p are the same as for o-Ps. The conversion rate γ is assumed to be three times that of o-Ps since p-Ps can be converted into three o-Ps states.

The positrons in the positronium which have formed a complex with a molecule will annihilate with a characteristic annihilation rate λ_m, and again practically all the annihilation takes place through 2γ annihilation.

When the probabilities of observing the positrons as p-Ps, o-Ps, free positrons or in a complex at a given time t, are P_s, P_t, P_f and P_m, the kinetic equations ruling these probabilities are

$$\frac{dP_s}{dt} = -(3\gamma + \lambda_s + \lambda_p + \lambda_o + \lambda_c)P_s + \gamma P_t \qquad (5.8)$$

$$\frac{dP_t}{dt} = -(\gamma + \lambda_t + \lambda_p + \lambda_o + \lambda_c)P_t + 3\gamma P_s \qquad (5.9)$$

$$\frac{dP_f}{dt} = -\lambda_f P_f + \lambda_o (P_s + P_t) \qquad (5.10)$$

$$\frac{dP_m}{dt} = -\lambda_m P_m + \lambda_c (P_s + P_t) \qquad (5.11)$$

In order to solve (5.8) and (5.9) we guess the following solutions

$$P_s = A \exp(-\lambda_1 t) + B \exp(-\lambda_2 t) \qquad (5.12)$$

$$P_t = C \exp(-\lambda_1 t) + D \exp(-\lambda_2 t) . \qquad (5.13)$$

Equations (5.8) to (5.13) were originally presented and solved by McGervey [21]. But since his solutions for λ_1, λ_2, A, B, C, D, P_f and P_m differ from the solutions presented here, a rather detailed presentation of the calculations will be given. Let us define

$$\lambda_s' = \lambda_s + \lambda_p + \lambda_o + \lambda_c \tag{5.14}$$

$$\lambda_t' = \lambda_t + \lambda_p + \lambda_o + \lambda_c . \tag{5.15}$$

Inserting (5.12) and (5.13) into (5.8) and (5.9) gives

$$-A\lambda_1 \exp(-\lambda_1 t) - B\lambda_2 \exp(-\lambda_2 t) = -(3\gamma + \lambda_s')\cdot (A\exp(-\lambda_1 t) + B\exp(-\lambda_2 t)) + \gamma(C\exp(-\lambda_1 t) + D\cdot\exp(-\lambda_2 t)) \tag{5.16}$$

$$-C\lambda_1 \exp(-\lambda_1 t) - D\lambda_2 \exp(-\lambda_2 t) = -(\gamma + \lambda_t')(C\exp(-\lambda_1 t) + D\exp(-\lambda_2 t)) + 3\gamma(A\exp(-\lambda_1 t) + B\exp(-\lambda_2 t)) . \tag{5.17}$$

Since these equations must be valid at all times, the coefficients to $\exp(-\lambda_1 t)$ must be independent of the coefficients to $\exp(-\lambda_2 t)$ and vice versa. Consequently the equations can be separated into equations only containing coefficients to $\exp(-\lambda_1 t)$ and only containing coefficients to $\exp(-\lambda_2 t)$. Disregarding the trivial solutions, the following equation is obtained for λ_1 or λ_2

$$\lambda_{1,2}^2 - \lambda_{1,2}(4\gamma + \lambda_t' + \lambda_s') + \gamma(3\lambda_t' + \lambda_s') + \lambda_t'\lambda_s' = 0 \tag{5.18}$$

yielding

$$\lambda_{1,2} = 2\gamma + \frac{\lambda_t}{2} + \frac{\lambda_s}{2} + \lambda_o + \lambda_p + \lambda_c \pm \sqrt{(4\gamma^2 + \lambda_s\gamma + \frac{(\lambda_s-\lambda_t)^2}{4} - \lambda_t\gamma)} . \tag{5.19}$$

A, B, C and D can be found from (5.16) and (5.17) together with the boundary conditions

$$A + B = P_s(0) \tag{5.20}$$

$$C + D = P_t(0) \tag{5.21}$$

yielding

$$A = C'(-P_s(0)\,B' + P_t(0)D')/N \tag{5.22}$$

$$B = D'(P_s(0)\,A' - P_t(0)C')/N \tag{5.23}$$

$$C = A'(-P_s(0)\,B' + P_t(0)D')/N \tag{5.24}$$

$$D = B'(P_s(0)\,A' - P_t(0)C')/N \tag{5.25}$$

where

$$A' = \lambda_1 - \lambda_s' \tag{5.26}$$

$$B' = \lambda_2 - \lambda_s' \tag{5.27}$$

$$C' = \lambda_t' - \lambda_1 \tag{5.28}$$

$$D' = \lambda_t' - \lambda_2 \tag{5.29}$$

$$N = A'D' - B'C' = (\lambda_1 - \lambda_2)(\lambda_t - \lambda_s) \ . \tag{5.30}$$

Note that $\lambda_t' - \lambda_s' = \lambda_t - \lambda_s$.

Equations (5.10) and (5.11) are differential equations of the following type

$$\dot{Y} + f(t)Y = g(t) \tag{5.31}$$

having the solution

$$Y = \exp(-\int f(t)dt)\ [\int g(t)\ \exp(\int f(t)dt)dt + C]. \tag{5.32}$$

Here C is an arbitrary constant that can be determined from the boundary conditions. Here

$$f(t) = \lambda_f \tag{5.33}$$

$$g(t) = \lambda_o(P_s + P_t) \tag{5.34}$$

for equation (5.10), and substituting λ_f for λ_m and λ_o for λ_c, we have the same equation for (5.11). In solving the above equations and integrals the following solutions are obtained:

$$P_f = \frac{\lambda_o(A+C)}{\lambda_f - \lambda_1}(\exp(-\lambda_1 t) - \exp(-\lambda_f t)) + \frac{\lambda_o(B+D)}{\lambda_f - \lambda_2}(\exp(-\lambda_2 t) - \exp(-\lambda_f t)) + \tag{5.35}$$

$$P_f(0)\exp(-\lambda_f t)$$

$$P_m = \frac{\lambda_c(A+C)}{\lambda_m - \lambda_1}(\exp(-\lambda_1 t) - \exp(-\lambda_m t) + \frac{\lambda_c(B+D)}{\lambda_m - \lambda_2}(\exp(-\lambda_2 t) - \tag{5.36}$$

$$\exp(-\lambda_m t)) + P_m(0)\exp(-\lambda_m t)$$

In a lifetime experiment we only measure the 2Y annihilation rate N(t):

$$N(t) = -\frac{d}{dt}(P_s + P_t + P_f + P_m) \tag{5.37}$$

and ignoring λ_t, which will not contribute to the 2Y annihilation,

$$N(t) = \lambda_s P_s + \lambda_f P_f + \lambda_m P_m + \lambda_p(P_s + P_t). \tag{5.38}$$

When a lifetime spectrum is analyzed it should, in principle, be possible to observe four different lifetimes λ_1, λ_2, λ_m and λ_f. In practice, however, λ_m and λ_f are so close to each other (both $2 - 3 \cdot 10^9\ s^{-1}$) that it is impossible to separate them in a lifetime spectrum.

A feature of the theoretical spectrum is the fact that negative intensities and intensities higher than 100% can occur. However, this does not violate any physical concept, as will be shown when some special cases are discussed. Anyhow, whenever one deals with an ordinary positron lifetime spectrum, it should be possible to set the irrelevant λ's and perhaps Y in equations (5.8) - (5.11) equal to zero, and then insert the relevant λ's in the presented solutions (5.12), (5.13), (5.19), (5.22) - (5.30) and (5.35), (5.36).

If, for instance, $\lambda_1 = \lambda_2$ it will be impossible to find A, B, C or D separately from the equations. But the physically meaningful concepts, such as A + B and C + D, can easily be found.

When Ps is formed in a liquid, the above description is insufficient to explain its behaviour. Since Ps is a very light particle it is difficult to confine it within a narrow region due to the zero point motion of the Ps. Consequently, Ps is supposed to blow itself some sort of a "bubble" in the liquid as pointed out by several authors[22, 23]. Also the electron blows

itself a bubble in some liquids[24, 25]. The bubble is, of course, only formed if the forces between the electron/Ps and the liquid are "sufficiently" repulsive. In order to perform analytical calculations on such a bubble, it is represented as a spherical potential well with infinite, high potential walls. Such a model is, of course, not correct, but it can give some quantitative ideas about bubble sizes and the reaction mechanism.

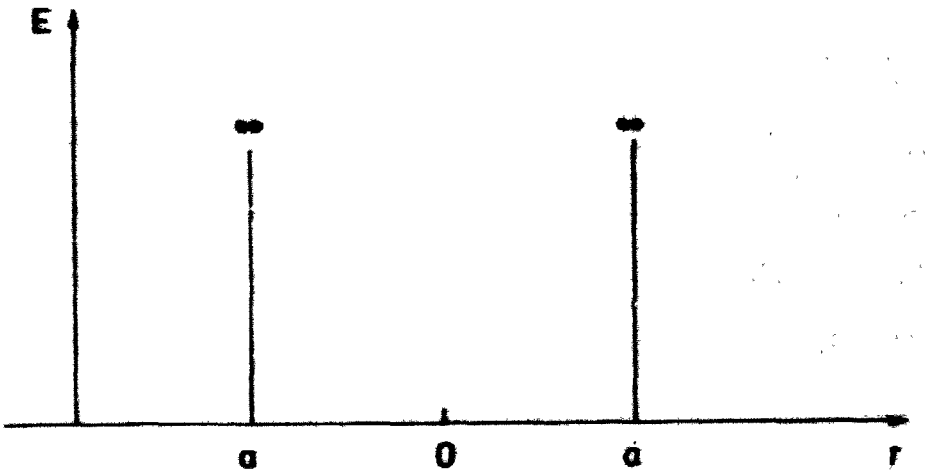

Fig. 11. The square well potential used to calculate the Ps energy in the bubbles in the liquids using formula (5.43).

The solution to the kinetic energy of a particle in such a three-dimensional potential can be found in several books on quantum mechanics and has been presented in ref. 22.

Setting $R(r) = \frac{\chi(r)}{r}$, and inserting in the Schrødinger equation, yields

$$\frac{-\hbar^2}{2m} \frac{d^2\chi(r)}{dr^2} = E\,\chi(r) \qquad \text{for} \quad r < a \qquad (5.39)$$

if we assume that the particle has no angular momentum. This corresponds to a particle in a one-dimensional potential where $\chi(r)$ has the following form

$$\chi(r) = A\sin(\alpha r) + B\cos(\alpha r) \qquad (5.40)$$

and

$$\alpha = \sqrt{\left(\frac{2mE}{\hbar^2}\right)} \; . \qquad (5.41)$$

Demanding that R(r) be finite for r=0, B must be zero. From the boundary condition $\chi(a) = 0$ we have

$$\alpha a = \frac{n\pi}{2} , \quad n \text{ even} . \tag{5.42}$$

Since $n = 0$ makes $\chi(r)$ identical to zero, the lowest acceptable solution is $n = 2$ giving

$$\alpha a = \pi \Rightarrow E_{kin} = \frac{\pi^2 \hbar^2}{4 m_e a^2} . \tag{5.43}$$

In order to calculate the bubble radii, it is necessary to evaluate what "sorts" of energy there are that are of importance to such a bubble; each of the energies are calculated separately. As an example we will use a bubble with a radius of 5 Å in a liquid with a surface tension of 20 dyn/cm and with an external pressure of 1 atm.

$$E_{kin} = \frac{\pi^2 \hbar^2}{4 m_e r^2} = 1.2 \cdot 10^{-12} \text{ erg} \tag{5.44}$$

$$E_{surface} = 4\pi r^2 \sigma = 6.3 \cdot 10^{-13} \text{ erg} \tag{5.45}$$

$$E_{PV} = P \cdot V = P \frac{3}{4} \pi r^3 = 5.3 \cdot 10^{-16} \text{ erg} \tag{5.46}$$

$$m_e = 9.1 \cdot 10^{-28} \text{ g}, \quad \hbar = 1.05 \cdot 10^{-27} \text{ erg s}, \quad 1 \text{ atm} = 1.01 \cdot 10^{9} \text{ erg}.$$

For small bubbles under atmospheric pressure it is justifiable to disregard the PV contribution to the energy and to set

$$E_{tot} = \frac{\pi^2 \hbar^2}{4 m_e r^2} + 4\pi r^2 \sigma . \tag{5.47}$$

Assuming that the bubble will have such a radius that its total energy will have a minimum, the radius of the bubble can be calculated.

$$\frac{dE}{dr} = \frac{-2\pi^2\hbar^2}{4m_e r^3} + 2 \cdot 4\pi r\sigma = 0 \quad \text{for}$$

$$r^4 = \frac{\pi\hbar^2}{16m_e\sigma} \Rightarrow r = \left(\frac{\pi\hbar^2}{16m_e}\right)^{1/4} \cdot \sigma^{-1/4} =$$

$$12.44 \cdot 10^{-8} \cdot \sigma^{-1/4}\ \text{cm} = 12.44 \cdot \sigma^{-1/4}\ \text{Å}, \qquad (5.48)$$

for $\sigma = 20$ dyn/cm, we have $r_b = 5.9$ Å.

To calculate a bubble radius of 5 Å by use of a macroscopically determined surface tension can seem rather crude. However, the approximations seem not unreasonable since different methods for determining the bubble size give radii not too far from each other.

The bubble sizes can also be determined from angular correlation measurements. In order to obtain mathematical solutions which can be treated by analytical methods, the Ps is in this case assumed to be in a three-dimensional harmonic potential. Under this assumption it is possible to calculate the bubble radius[16]. The potential can be written

$$V = m_e \omega^2(x^2 + y^2 + z^2) \qquad (5.49)$$

where ω is the classical frequency of the harmonic oscillator. Here the ground state wavefunction can be separated into three independent functions. In this case only the z dependence of the wavefunction is of interest.

$$\psi(z) = N_z \exp\left(-\frac{m_e\omega z^2}{\hbar}\right). \qquad (5.50)$$

Here all N's are normalization constants. The probability distribution along the z direction is

$$|\psi(z)|^2 = N_z^2 \exp\left(-\frac{2m_e\omega z^2}{\hbar}\right). \qquad (5.51)$$

The FWHM (Γ_z) of 5.51 is

$$\Gamma_z = \left(\frac{2\hbar\ln 2}{m_e\omega}\right)^{1/2}. \qquad (5.52)$$

The Fourier transform of $\psi(z)$ determines the distribution of p_z, the z component of the momentum

$$\psi(p_z) = N' \int_{-\infty}^{\infty} \exp\left(- \frac{m_e \omega z^2 + i p_z z}{\hbar} \right) dz = N'' \exp\left(- \frac{p_z^2}{\hbar 4 m_e \omega}\right). \tag{5.52}$$

The p_z probability distribution is

$$|\psi(p_z)|^2 = N''^2 \exp\left(- \frac{p_z^2}{2\hbar m_e \omega}\right) . \tag{5.53}$$

Remembering that in an angular correlation experiment the correlation between θ and p_z is

$$\theta = \frac{p_z}{m_e c} , \tag{5.55}$$

we have

$$\Gamma_\theta \Gamma_z = \frac{4\hbar \ln 2}{m_e c} = 10.7 \text{ (m rad} \cdot \text{Å)}, \tag{5.56}$$

where Γ_θ is the FWHM of the θ distribution.

This means that having a given Γ_θ, Γ_z can be calculated using equation (5.56). The Γ_θ can be obtained from the angular correlation curve for positrons and Ps in the organic liquid. The p-Ps normally annihilate through intrinsic annihilation and the FWHM of the narrow peak in the angular correlation spectrum will be roughly inversely proportional to the FWHM of the p-Ps z probability distribution. The resolution of the apparatus (Γ_{ap}) will, of course, also contribute to the FWHM of the narrow component in the angular correlation curve. The measured FWHM (Γ_m) of the narrow peak from p-Ps is

$$\Gamma_m^2 = \Gamma_{ap}^2 + \Gamma_\theta^2 \Rightarrow \Gamma_\theta = (\Gamma_m^2 - \Gamma_{ap}^2)^{1/2} \tag{5.57}$$

Here it is assumed that the p_z -, the θ distribution, and the apparatus resolution function can be approximated by Gaussians.

From the Γ_z is is easy to obtain the radius within which 90% of the Ps is confined. This radius is called the bubble radius (R_b). From a table of normal probabilities we have

$$\frac{1}{\sigma\sqrt{\pi}} \int_{-x}^{x} \exp(-(\frac{t}{\sigma})^2)dt = 0.9 \quad \text{for } x = 1.645 . \tag{5.58}$$

Recalling that $|\phi(z)|^2 = N_z^2 \exp(- \frac{4 \ln 2}{\Gamma_z^2} z^2)$

we have, by combining (5.58), (5.51) and (5.56),

$$R_b = \frac{1.645\, \Gamma_z}{\sqrt{4 \ln 2}} = 0.988 \quad \Gamma_z . \tag{5.59}$$

This shows that R_b is very close to Γ_z. The bubble radii calculated using (5.59), (5.56) and (5.48) are presented in table 7.1. The harmonic potential was used in (5.56) and (5.59), because it was not possible to separate the wavefunction for the square well potential into three independent wavefunctions. Consequently, it was not simple to calculate $\Gamma_z \Gamma_\theta$ for the square well potential.

The belief that the Ps is contained in a bubble in an organic liquid complicates the reaction mechanism between Ps and electron acceptors, as shown by Goldanskii and Shantarovich in ref. 5. Here a very simple model is proposed in order to visualise what is believed to be the reaction mechanism in the bubble. The total Ps potential is illustrated on fig. 12.

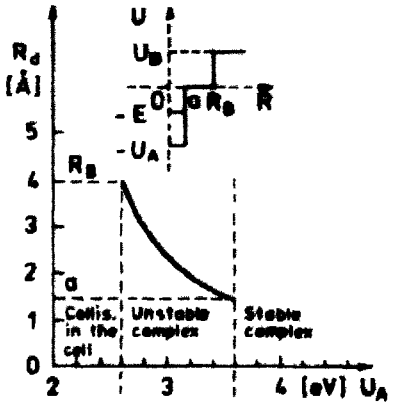

Fig. 12. The combined electron acceptor, bubble potential for Ps in a liquid containing electron acceptors. This potential is used in (5.60) in calculating the Ps energy. The thickly drawn slope shows the bubble radius (R_d) for which the Ps leaves the acceptor as a function of the acceptor potential depth. In the example used, U_B = 1 eV and a = 1.5 Å. Ref. 5.

Here the depth of the potential well in the liquid is U_B and the radius of the bubble R_B. The depth of the potential of the acceptor is U_A and the radius of the acceptor is a. In such a potential, Shantarovich found the relation between R, the actual radius of the bubble, a, U_A, U_B and E the energy of Ps in this complex to be

$$R - a = \frac{1}{2\zeta_E} \ln \frac{\sqrt{|E|} - \sqrt{U_B + |E|}}{\sqrt{|E|} + \sqrt{U_B + |E|}} \cdot \frac{\sqrt{|E|} - \sqrt{U_A - |E|}\cot\sqrt{\zeta_A^2 - \zeta_E^2}\, a}{\sqrt{|E|} + \sqrt{U_A - |E|}\cot\sqrt{\zeta_A^2 - \zeta_E^2}\, a} \tag{5.60}$$

$$\zeta_E = \frac{2}{\hbar}\sqrt{m_e|E|}\,, \qquad \zeta_A = \frac{2}{\hbar}\sqrt{m_e U_A}\,.$$

A crude description of the contents of this equation can be given as follows. $|E|$ increases with increasing a, and also increases with increasing R_B. Descrease of a can result in a decrease of $|E|$ to such an extent that the Ps leaves the complex. Decrease of R_B can also result in such an increase in the Ps energy that the Ps leaves the complex. The critical radius (R_d) for which the Ps can leave the acceptor was calculated by Shantarovich to be[5]

$$R_d = a + \frac{1}{\zeta_A \tan(\zeta_A a - \pi/2)} - \frac{1}{\zeta_B}$$

$$\zeta_B = \frac{2}{\hbar}\sqrt{m_e U_B}\,. \tag{5.61}$$

An increase of $|U_A|$ will result in an increase of $|E|$.

Two typical Ps, electron acceptor reactions in an organic liquid will be described. The Ps diffuses around in a bubble until it reaches a strong acceptor. The Ps becomes attached to the acceptor by an energy E. Since the Ps is now chemically bound to the acceptor, it ceases to exert a pressure on the bubble walls and the bubble shrinks. During this shrinking $|E|$ decreases, but assuming $|U_A|$ to be large enough, the Ps remains on the acceptor and annihilates with a characteristic annihilation rate λ_m. In this case the bubble does not affect the reaction mechanism. If, however, $|U_A|$ had been rather small, the Ps attachment to the acceptor could have taken place as in the previous case, but during the shrinkage of the bubble the Ps would have obtained a positive energy and left the acceptor. During the time that the Ps was on the acceptor, it would have an annihilation rate

of λ_m, and while the Ps is in the bubble the annihilation rate would be λ_p. Here much of the Ps which was attached to the acceptor would leave the acceptor again as Ps. The mechanism of being attached to the acceptor and then leaving it again and returning to the solvent must be incorporated into the kinetic equations. The parameter that determines what length of time the Ps remains on the acceptor is the time that it takes for the bubble to shrink from its original radius R_B to the radius R_d where the Ps leaves the acceptor. This time will depend on $R_B - R_d$ and the shrinkage velocity (v_s) of the bubble. This velocity is[26]

$$v_s = \frac{\sigma}{2\eta} , \tag{5.62}$$

where η is the viscosity of the liquid. For organic liquids this velocity will normally be in the interval 0.05 - 1 Å/ps. Finally, U_A can be so small that the Ps cannot become attached to the acceptor and no quenching is observed.

The kinetic equations for the quenching of o-Ps will be presented both with and without the possibilities of Ps leaving the acceptor, at first for Ps complex formation in a stable complex. This equation can be obtained from equations (5.9) and (5.11) setting $Y = \lambda_t = \lambda_o = 0$

$$\frac{dP_t}{dt} = -(\lambda_p + \lambda_c) P_t ; \qquad P_t(0) = 1 \tag{5.63}$$

$$\frac{dP_m}{dt} = -\lambda_m P_m + \lambda_c P_t ; \qquad P_m(0) = 0 \tag{5.64}$$

Here

$$\lambda_1 = \lambda_2 = \lambda_p + \lambda_c$$

$$P_t = \exp(-(\lambda_p + \lambda_c)t) \tag{5.65}$$

$$P_m = \frac{\lambda_c}{\lambda_m - \lambda_p - \lambda_c} (\exp(-(\lambda_p + \lambda_c)t) - \exp(-\lambda_m t)) . \tag{5.66}$$

What we measure is:

$$N(t) = -\frac{d}{dt}(P_m + P_t) = I_1 \lambda_m \exp(-\lambda_m t) + I_2(\lambda_p + \lambda_c) \exp(-(\lambda_p + \lambda_c)t) \tag{5.67}$$

$$I_1 = \frac{-\lambda_c}{\lambda_m - \lambda_p - \lambda_c} \; ; \qquad I_2 = \frac{\lambda_m - \lambda_p}{\lambda_m - \lambda_p - \lambda_c} \; . \tag{5.68}$$

Here it is interesting that for $\lambda_c \neq 0$, I_1 is negative and $I_2 > 1$. $\lambda_c = 0$ corresponding to $[A] = 0$ giving normal pick-off annihilation of the o-Ps. As $[A]$ increases, λ_c increases; I_2 increases towards infinity as $\lambda_c \to \lambda_m - \lambda_p$. At the same time I_1 goes toward minus infinity. The o-Ps lifetime spectra for some special cases are shown on fig. 13.

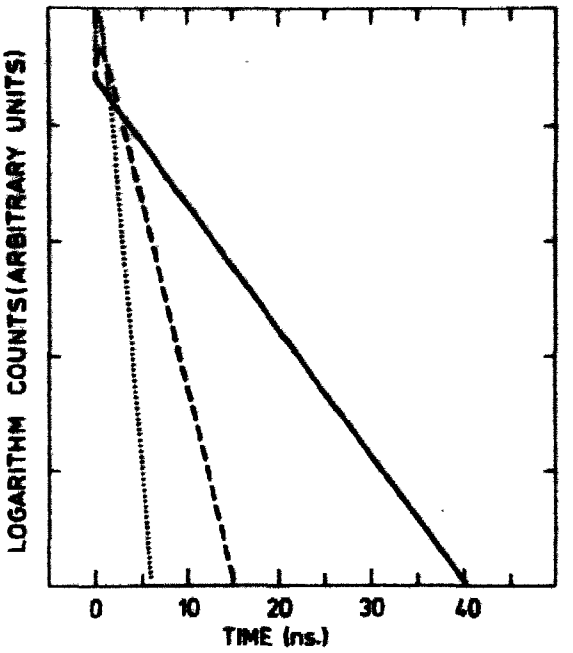

Fig. 13. Calculated o-Ps lifetime spectra. The spectra are calculated by using formula (5.67). The curves all have $\lambda_1 = \lambda_m = 2.5 \cdot 10^9\ s^{-1}$. For the fully drawn curve, $\lambda_2 = \lambda_p + \lambda_c = (0.25 + 0) \cdot 10^9\ s^{-1}$, $I_1 = 0\%$ and $I_2 = 100\%$. For the dashed curve, $\lambda_2 = 0.75 \cdot 10^9\ s^{-1}$, $I_1 = -28.57\%$ and $I_1 = 128.57\%$. For the dotted curve, $\lambda_2 = 2.45 \cdot 10^9\ s^{-1}$, $I_1 = -4400\%$ and $I_2 = 4500\%$.

The physical explanation of the spectra containing negative intensities is the following. At $t = 0$ all the o-Ps is in the solvent where it annihilates with λ_p, as time goes on more and more o-Ps forms a complex where it annihilates with λ_m; λ_m is often ten times as large as λ_p. For small times this will give rise to an increase in the annihilation rate as the times increase.

After some time, the total amount of Ps decreases to such an extent that the annihilation rate decreases due to the decreased amount of Ps.

Thus, in a lifetime experiment where o-Ps is quenched, one cannot set the amount of o-Ps formed equal to the intensity of the longest-lived component. The original amount of o-Ps can be calculated if the intensity of the longest-lived component, λ_p, λ_m and λ_c are known. Normally the intensity, λ_p and λ_c, is known from the analyzed spectra. The intensity is given by the computer. $\lambda_p = \tau_p^{-1}$, where τ_p is the o-Ps lifetime in the pure solvent and $\lambda_c = \tau_{p'}^{-1} - \tau_p^{-1}$ where $\tau_{p'}$ is the o-Ps lifetime in the solvent with quencher present. λ_m is, however, practically always unknown, but it is believed to be close to the λ_f of free positrons. The reason for assuming this is that practically all lifetime spectra of organic solvents with quencher present can be fitted with only three lifetimes, and good fits (variance ~ 1) can be obtained. Here the shortest lifetime τ_1 is believed to arise from p-Ps $\tau_1^{-1} = \lambda_s + \lambda_p + \lambda_c$. The median lifetime τ_2 is believed to arise from λ_f and λ_m. This lifetime is normally 0.3 - 0.5 ns and cannot be separated into two independent components. Finally, we have the longest lifetime τ_3, which is ascribed to o-Ps $\tau_3^{-1} = \lambda_p + \lambda_c$. If λ_m was very different from τ_1^{-1}, τ_2^{-1}, or τ_3^{-1}, it would cause poor fits, and a significant improvement of the fits when a three-lifetime fit was extended to a four-lifetime fit. This improvement of the fit is not obtained normally.

The next equations to be solved are those for o-Ps complex formation and splitting up of the complex due to bubble shrinkage.

$$\frac{dP_t}{dt} = -\lambda_p P_t - \lambda_c P_t + \lambda_c k' P_t (t-t_o) \qquad (5.69)$$

for $t \geq t_o$

$$\frac{dP_m}{dt} = -\lambda_m P_m + \lambda_c P_t - \lambda_c k' P_t (t-t_o) \qquad (5.70)$$

$$k' = \exp(-\lambda_m t_o) . \qquad (5.71)$$

t_o is the time it takes the bubble to shrink from R_B to R_d ($t_o = (R_B - R_d)/v_s$) where the Ps leaves the acceptor. Equations (5.69) and (5.70) are equal to equations (5.63) and (5.64), except for the term $\lambda_c k' P_t (t-t_o)$. This term takes care of the Ps leaving the complex. $k' = \exp(-\lambda_m t)$ determines the fraction of the positrons which formed a complex t_o ago and which is still not annihilated from the complex state with λ_m. After t_o all this Ps will

again leave the complex due to bubble shrinkage. For $t_o = 0$, $\lambda_c P_t$ and $\lambda_c k' P(t-t_o)$ cancel each other, which means that no quenching is observed. For $t_o \to \infty$, $k' \to 0$ and (5.69) and (5.70) are reduced to (5.63) and (5.64). As a trial solution is used

$$P_t = A \exp(-\lambda_1 t) + B \exp(-\lambda_2 t) \tag{5.72}$$

$$P_m = C \exp(-\lambda_1 t) + D \exp(-\lambda_2 t) . \tag{5.73}$$

Inserting (5.72) and (5.73) into (5.69) and (5.70) gives the following equations for λ_1 and λ_2:

$$-\lambda_1 + \lambda_p + \lambda_c - \lambda_c k' \exp(\lambda_1 t_o) = 0 \tag{5.74}$$

$$-\lambda_2 + \lambda_p + \lambda_c - \lambda_c k' \exp(\lambda_2 t_o) = 0 \tag{5.75}$$

$$(-\lambda_1 + \lambda_m) C + (-\lambda_c + \lambda_c k' \exp(\lambda_1 t_o))A = 0 \tag{5.76}$$

$$(-\lambda_2 + \lambda_m)D + (-\lambda_c + \lambda_c k' \mathrm{esp}(\lambda_2 t_o))B = 0 . \tag{5.77}$$

In order to obtain two different solutions for λ_1 and λ_2, B is set equal to zero, giving

$$\lambda_2 = \lambda_m \tag{5.78}$$

$$-\lambda_1 + \lambda_p + \lambda_c - \lambda_c k' \exp(\lambda_1 t_o) = 0 . \tag{5.79}$$

Here $\lambda_2 = \lambda_m$ corresponds to the solution from (5.63) and (5.64). In (5.79) λ_1 is no longer a linear parameter and λ_1 can only be found using numerical methods. Since the equation is differential, the solution to (5.79) can easily be found using the Newton iteration method. In this case λ_1 corresponds to $\lambda_p + \lambda_c$ for the quenching case without bubble effects. From the boundary conditions

$$A + B = P_t(0); \quad B = 0 \quad A = P_t(0) = 1 \tag{5.80}$$

$$C + D = P_m(0); \quad P_m(0) = 0 \quad C = -D \tag{5.81}$$

(5.74) and (5.76) give

$$(\lambda_p-\lambda_1) + C(\lambda_m-\lambda_1) = 0, \Rightarrow C = \frac{\lambda_1-\lambda_p}{\lambda_m-\lambda_1} . \qquad (5.82)$$

We measure

$$N(t) = - \frac{d}{dt}(P_t+P_m) = I_1\lambda_1 \exp(-\lambda_1 t) + I_2\lambda_m \exp(-\lambda_m t) \qquad (5.83)$$

where, from (5.72) and (5.73),

$$I_1 = A + C = \frac{\lambda_m-\lambda_p}{\lambda_m-\lambda_1} \qquad (5.84)$$

$$I_2 = -C = \frac{\lambda_p-\lambda_1}{\lambda_m-\lambda_1} . \qquad (5.85)$$

In order to find C, the two limits for λ_1 are determined.

For $\lambda_c = 0$, $\lambda_1 = \lambda_p$.

Rewriting (5.74) gives

$$-\lambda_1 + \lambda_p + \lambda_c - \lambda_c \exp((\lambda_1-\lambda_m)t_o) = 0 \qquad (5.74)$$

λ_1 increases with increasing λ_c and $\exp((\lambda_1-\lambda_m)t_o)$ can be expanded for small $(\lambda_1-\lambda_m)t_o$, yielding

$$-\lambda_1 + \lambda_p + \lambda_c (1-1-\lambda_1 t_o + \lambda_m t_o) = 0.$$

In solving for λ_1 we have

$$\lambda_1 = \frac{\lambda_p+\lambda_c \lambda_m t_o}{1+\lambda_c t_o} \rightarrow \lambda_m \quad \text{for} \quad \lambda_c \rightarrow \infty . \qquad (5.86)$$

From this it can be seen that

$\lambda_m \geq \lambda_1 \geq \lambda_p$ giving

$I_1 \geq 1$ and goes toward ∞ for $\lambda_1 \rightarrow \lambda_m$, and

$I_2 \leq 0$ and goes toward $-\infty$ for $\lambda_1 \rightarrow \lambda_m$.

One must recall that when comparing o-Ps quenching with and without bubble effects both cases give an annihilation rate λ_m associated with an intensity going from zero to minus infinity. Both cases also give an annihilation rate going from λ_p and upwards associated with an intensity going from 1 towards infinity. Although the "smallest" λ for the bubble case is limited to λ_m, and will always have a positive intensity, it can in principle, without bubble effects, go towards infinity and be associated with a negative intensity.

Without bubble effects the λ corresponding to τ_3 would be (5.67)

$$\lambda = \lambda_p + \lambda_c = \lambda_p + k\,[A] \qquad (5.87)$$

from where the rate constant (k) could be found.

$$k = \frac{\lambda - \lambda_p}{[A]} \,. \qquad (5.88)$$

In order to see whether or not one will obtain a rate constant (k_r)

$$k_r = \frac{\lambda_1 - \lambda_p}{[A]} \,, \qquad (5.89)$$

which in reality is a constant in cases where bubble effects are of importance, k_r has been found from λ_1 in solving (5.79) for different t_o. Typical values of t_o will be from 4-80 ps, assuming typical shrinking radii from 6 to 2 Å and shrinking velocities from 0.05-1 Å/ps. The result for $\tau_1 = \lambda_1^{-1}$ and k_r is shown on figs. 14 and 15. Here it can be seen that, although the reaction mechanism and the kinetic equations differ with and without bubble effects, the solutions to these two kinds of equation resemble each other to a large extent. The effective rate constant with bubble effects seems to be a constant over a large concentration range. This means that making a single measurement on a quencher does not give direct information about whether or not bubble effects are of importance for the reaction.

After a study of the kinetic equations, other phenomena of importance for the lifetime spectra will be discussed. The pick-off annihilation rate has been investigated.

Levay and Hautojärvi[27] proposed a model stating additivity of the pick-off annihilation probabilities in mixtures AB of two liquids A and B

$$V_{AB}\,\lambda_{AB} = \lambda_A V_A - (\lambda_A V_A - \lambda_B V_B) X_B \,, \qquad (5.90)$$

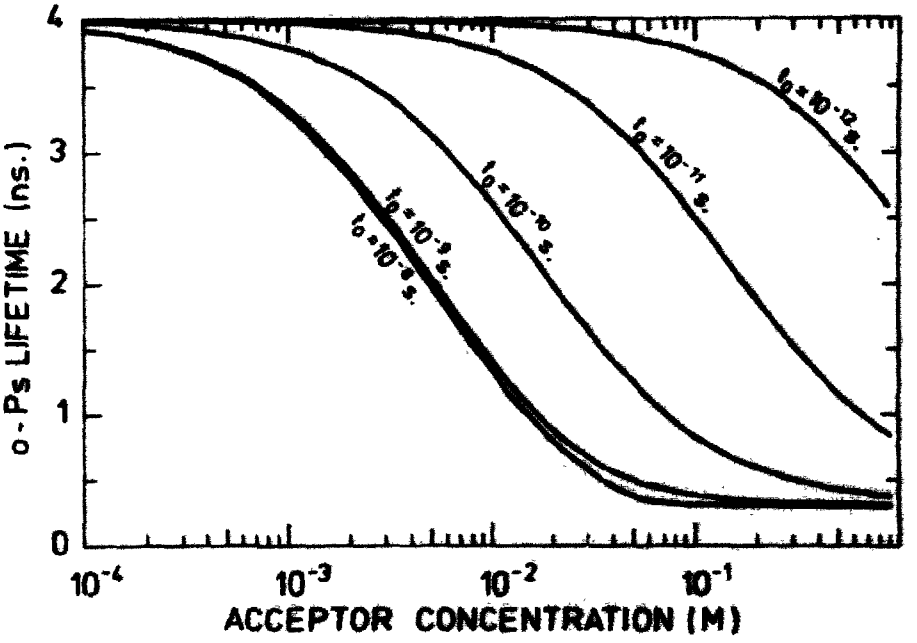

Fig. 14. o-Ps lifetimes calculated using formula (5.79). In these calculations $\lambda_c = 5 \cdot 10^{10}$ [A] s^{-1}, $\tau_p = \lambda_p^{-1} = 4$ ns, $\tau_m = 0.3$ ns. t_0 is the time from the o-Ps is attached to the acceptor and until it leaves the acceptor due to bubble shrinkage.

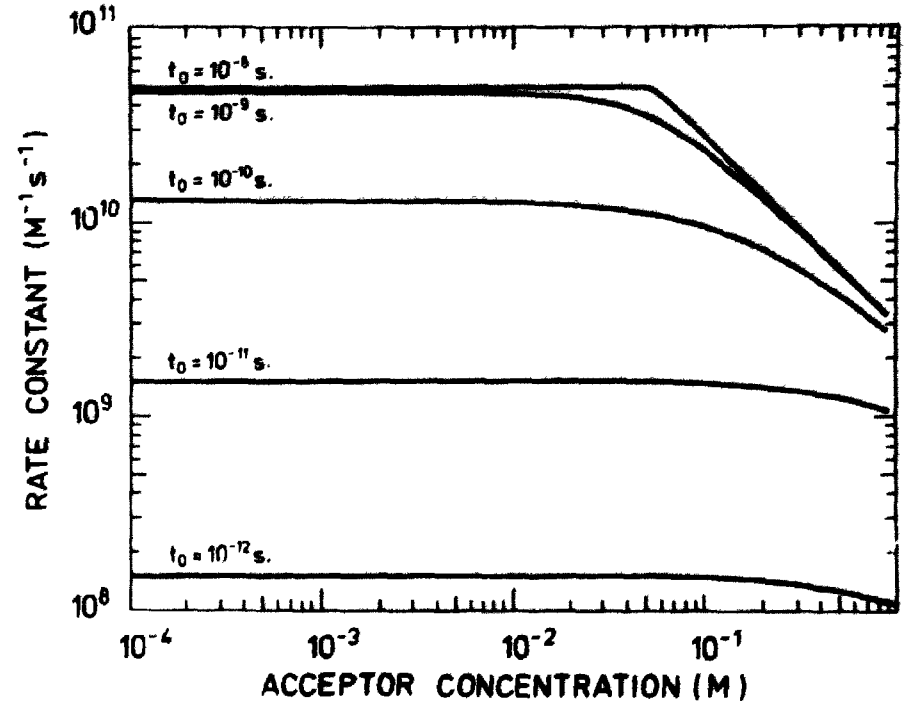

Fig. 15. The rate constant calculated using formulae (5.89) and (5.79). The values for τ_p, τ_m, and λ_c are the same as used for fig. 14.

where λ is the pick-off annihilation rate, V the molar volume, and X the mole fraction. Later the same authors, together with Vertes[28], modified the model to

$$V_{AB}\sqrt{\lambda_{AB}} = V_A\sqrt{\lambda_A} - (V_A\sqrt{\lambda_A} - V_B\sqrt{\lambda_B})X_B . \qquad (5.91)$$

The same formulas expressed in lifetimes $\tau = \lambda^{-1}$ and volume percentages a, b are

$$\tau_{AB} = 10^2\ \tau_A/(100 - b + b\ \tau_A/\tau_B) \qquad (5.90a)$$

$$\tau_{AB} = 10^4\ \tau_A/(100 - b + b\sqrt{\tau_A/\tau_B})^2 . \qquad (5.91a)$$

Also Tao[29] proposed a simple model for the pick-off annihilation rate in liquids, stating

$$\lambda = \alpha\gamma^{\nu} \qquad (5.92)$$

where γ is the surface tension and α, ν are constants to be fitted.

Results referring to (5.90) and (5.91) will be presented and discussed in section 7.

A topic of major importance for the Ps lifetime - and angular correlation spectra - concerns what sorts of reactions and parameters determine the Ps formation probability.

Recently Mogensen published a new model of positronium formation: the spur reaction model[10]. Positronium is assumed to be formed by a reaction between a spur electron and the positron in the positron spur. The positron spur is the group of reactive intermediates (the positron, electrons, positive ions, etc.) which is created when the positron loses the last amount of its kinetic energy. Ps formation must compete with electron-ion recombination, with any electron and positron reaction with solvent molecules and scavengers, and with electron or positron diffusion out of the spur. It is also influenced by electron and positron solvation and by other changes in the properties of the spur. The model indicates a correlation of the Ps formation probabilities and the properties of the electron spurs studied in radiation chemistry[30]. Some aspects of the spur model will be discussed in rather more detail in sectin 8.

Until very recently the only model of Ps formation used was the Ore model[31], or a modified version of it. In this model it is assumed that during slowing down the positron may only form Ps in a certain energy

interval which is roughly $V-V_p \leq E \leq V$, where V is the ionization energy of the molecules and V_p (= 6.8 eV) is the ionization energy of Ps. Below $V-V_p$ a positron cannot pick-off an electron from the molecules to form Ps for energy reasons. Above roughly V ionization of the molecules is assumed to be more probable than Ps formation. The Ps atoms are then formed with kinetic energies $0 \leq E \leq V_p$, and they may undergo reactions before being thermalized[32-36]. Compounds which can only react with "hot" Ps will cause a reduction in I_3, thereby reducing the apparent Ps formation probability $P = 4/3\ I_3$ if no Ps quenching takes place. I_3 is the intensity of the longest-lived component. The Ore model with the addition of "hot" Ps-reactions has been the accepted model of Ps formation for several years. The parameters of the modified Ore model (thermalization cross sections, ionization energies, etc.) are nearly always unknown. Hence, by a suitable choice of these parameters, this model can reproduce almost any Ps formation probabilities measured. The author of the present work, however, favours the spur reaction model, which can be qualitatively or semi-quantitatively tested by use of radiation chemistry data.

Several of the measurements presented were performed on solutions containing charge-transfer (CT) complexes, and for this reason a short description of CT-complexes will be given. A CT-complex is a complex between an electron acceptor (A) and an electron donor (D). An electron acceptor can be defined as an atom or molecule with a positive electron affinity (EA)

$$EA = E(A) - E(A^-), \qquad (5.93)$$

where E(A), ($E(A^-)$) is the total energy of the acceptor (negatively charged acceptor). An electron donor is a molecule with low ionization potential.

The binding energy of a CT-complex arises from a partial transferring of charge from the highest occupied molecular orbital (HOMO) of the donor to the lowest empty molecular orbital (LEMO) of the acceptor. The CT-complex molecular orbitals (MO) are often written as linear combinations of the unperturbed MO of the acceptor and the donor extended to include the MO of the negatively charged acceptor and the positively charged donor.

The donors and acceptors are normally named according to the type of MO donating or accepting the electrons. Increvalent donors are lone-pair (n-) donors such as amines, ethers and alcohols. Sacrificial donors are compounds donating an electron from a bonding orbital. They include σ-donors, such as hydrocarbons, and π-donors such as aromatic compounds.

Usually the σ donors are weak donors, whereas the n- and π-donors can be rather good donors. Sacrificial acceptors can be of σ- or π-type. Hydrogen halides are examples of σ-acceptors and molecules containing double bonds close to electronegative substituents, e.g. halogens, nitro or cyano groups, are examples of π-acceptors.

When an electron donor and an acceptor collide they can form a CT-comples (AD), this complex can again split up in forming A and D. The complex formation velocity is $k_1[A][D]$ and the disintegration velocity is $k_2[AD]$, where k_1, k_2 are rate constants. These two velocities are equal to each other in equilibrium

$$[A][D]k_1 = [AD]k_2$$

$$\frac{[AD]}{[A][D]} = \frac{[AD]}{([A_o] - [AD])([D_o] - [AD])} = \frac{k_1}{k_2} = K, \qquad (5.94)$$

where K is the complexity constant, [AD] the CT complex concentration and $[A_o]([D_o])$ is the total acceptor (donor) molecule concentration, regardless of whether it is free or in a complex. Rewriting eq. (5.94) we get for the complex concentration

$$[AD] = 1/2\left[[A_o] + [D_o] + K^{-1} - \sqrt{([A_o] + [D_o] + K^{-1})^2 - 4[A_o][D_o]} \right] \qquad (5.95)$$

and hence for the free acceptor concentration

$$[A] = [A_o] - [AD]. \qquad (5.96)$$

If a CT complex and an acceptor are both present, the kinetic equations have to be modified. The o-Ps annihilation rate

$$\lambda = \lambda_p + k[A]$$

has to be extended to

$$\lambda = \lambda_p + k[A] + k_1[AD] \qquad (5.97)$$

where $k(k_1)$ are rate constants for the acceptor (CT-complex).

In principle it should be possible from the spur reaction model[10] to obtain a theoretical expression for the Ps yield as function of electron scavenger (acceptors and CT-complexes) concentration. The model predicts

that the presence of an electron scavenger decreases the Ps yield simply because some of the spur electrons, which would otherwise have contributed to the Ps formation, react with the scavenger. The concentration dependence of this scavenging process can principally be calculated by use of the diffusion models of the positron spur. The problems involved in this are discussed in some detail in ref. 37. The conclusion is that since there are no well-established models for electron scavenging, no reliable expression for the Ps yield can be obtained, and only qualitative correlations between Ps yields and radiation chemistry results can be made. In order to roughly describe the Ps yield results by a few parameters, we choose (as in ref. 37) to use the formula proposed by Green and Bell[38] for the Ps yield P, extended to include two inhibiting species

$$P = P_o/(1 + \sigma[A] + \sigma_1[AD]), \tag{5.98}$$

where P_o is the yield in the pure solvent and σ (σ_1) may be called the inhibition constant for the acceptor (CT complex).

Combining eqs. (5.68) and (5.98), we get for the relative intensity of the long-lived component

$$I = \frac{I_o(\lambda_m - \lambda_p)}{(\lambda_m - \lambda_p - \lambda_c)(1 + \sigma[A] + \sigma_1[AD])} \tag{5.99}$$

where I_o is the o-Ps intensity in the pure solvent.

The model proposed by Green and Bell is based on the following assumptions. During and/or after slowing down the positron can undergo reactions. Some lead to Ps formation P_{Ps} and some do not lead to Ps formation P_{ot}. In adding a compound [C], which decreases Ps formation (Ps inhibition), a new reaction is introduced that does not lead to Ps formation. The probability for this process P_c is assumed to be proportional to the concentration of C. The total Ps formation probability P is then

$$P = \frac{P_{Ps}}{P_{Ps} + P_{ot} + \alpha[C]},$$

where α is a constant. This equation can be rewritten

$$P = \frac{P_o}{1 + \sigma[C]}. \tag{5.100}$$

The optical spectra used to determine some CT-complex constants were fitted by

$$Abs = \varepsilon l[A] + \varepsilon_1 l[AD], \qquad (5.101)$$

here Abs is the absorbance, l the length of the cell and ε, ε_1 the extinction coefficients for the acceptor and the complex. [A] and [AD] are given by eqs. (5.95) and (5.96). The program used for fitting the optical data is described in more detail in appendix 1. References 39-45 give further information on CT-complexes.

6. EXPERIMENTAL

All samples for the angular correlation measurements, as well as for lifetime measurements, were degassed before the measurements were performed. This was done in order to remove the oxygen from the samples. Oxygen is an electron acceptor and reacts with Ps. This causes a shortening of the Ps lifetime and a decrease of the intensity in the narrow peak in the angular correlation curves, due to p-Ps which becomes oxidized or forms a complex with the oxygen.

For tetracyanoethylene (TCNE) and hexamethylbenzene (HMB) in dioxane, and 1-pyridiniumpropanesulfonate-3' (PPS) in water the oxygen in the solvents was removed by bubbling Ar through the solvents. All other liquids were degassed by the freeze-thaw method and afterwards distilled in vacuum into an ampoule. For samples intended for lifetime measurements, the positron source was contained in this ampoule. During recording of the lifetime spectra, the source and the sample were kept in this airtight ampoule. The positron source was kept outside the sample ampoule for the angular correlation measurements.

With the exception of pyrrolidine, all liquids were of puriss. p.a. and spectroc. grade. They were used without further purification. The pyrrolidine was of prac. grade. This liquid was distilled and only the median fraction, containing roughly 50% of the original volume, was used.

The iodine was of puriss. p.a. grade and used without further purification. The TCNE was purified by sublimation, the HMB was of purum grade and used without further purification. Later, a Ps lifetime spectrum with recrystallized HMB gave the same results as one of the presented spectra. The tetracyanoquinodimethane (TCNQ) was recrystallized from CH_3CN. An IR gas spectrum of the SO_2 showed no impurities and the trimethylamine (TMA) was distilled before use.

The concentrations in the solutions containing SO_2 and TMA were determined by condensing the SO_2 or TMA in an ampoule containing a known amount of solvent. The amount of SO_2 or TMA was determined by PV technique. The PV technique was also used to determine the concentration of SO_2 and TMA in the solutions containing SO_2-TMA complex.

The gas phase complexity constant between SO_2 and TMA was also determined by use of PV technique. To the knowledge of the author, this was the first time that this direct method was used to determine complexity constants. It is shortly discussed in appendix II.

The oxygen concentration in n-heptane was determined by PV technique by degassing an oxygen saturated n-heptane solution.

For the nitrobenzene and iodine in alkanes, and for CS_2 in tetramethylsilane (TMS), neopentane, isooctane and tetradecane and O_2 in n-heptane, all spectra were analyzed for three lifetimes and three intensities. The spectra were analyzed with the new and extended version of the program POSITRONFIT[19]. The positron source was enclosed between two capton foils in which 8.5% of the positrons annihilated. The lifetime spectra of the positrons annihilating in the foils is composed of two lifetimes of 0.391 ns with an intensity of 99.6% and a lifetime of 4.032 ns with an intensity of 0.4%. This spectrum was calculated and subtracted from the original spectra before final analysis of the lifetime spectra.

For CS_2 in n-hexane and for pyrrolidine, dioxane, and triethylamine (TEA) in n-heptane, about 45μCi ^{22}NaCl deposited between two Ni foils of 3.7 mg/cm^2 was used as the positron source. The spectra were analyzed with a new and extended version of the program POSITRONFIT[19] for three lifetimes and intensities. 20% of the positrons annihilated in the Ni foils where 95% of them had a lifetime of 0.2 ns and 5% had a lifetime of 2 ns. The spectrum of the positrons annihilating in the foils was calculated and subtracted from the original spectra before the final analysis.

For the rest of the lifetime spectra presented, ^{22}NaCl deposited between two Ni foils of approx. 4 mg/cm^2 was used as the positron source. The spectra were analysed by the POSITRONFIT program[18] for three lifetimes and intensities. Only for SO_2 in n-heptane was a correction carried out for some of the positrons annihilating in the source. Here a long-lived tail with a lifetime of 2.4 ns and an intensity of 0.7% was removed before analysis of the spectra. In order to separate the median lifetime and the longest lifetime for SO_2 in dioxane, the median lifetime was fixed at 500 ps. Hence only two lifetimes and three intensities were free in the final analysis. The 500 ps was the average median lifetime when the same spectra were analyzed for three lifetimes and three intensities.

The angular correlation spectra of the pure liquids were analyzed with the program PAACFIT[20] for three FWHM's and three intensities.

7. RESULTS

The results obtained from the PAT measurements are presented in this section, and more detailed discussion of them is given in section 8.

First, we present some radii of the bubbles formed by Ps in different organic solvents. These radii are calculated from the surface tension of the liquids and from the FWHMs of the narrow component in the angular correlation curve. The narrow component is believed to arise from the intrinsic p-Ps annihilation.

The next results to be presented are the rate constants for the reaction between o-Ps and iodine in different alkanes and nitrobenzene in different alkanes. For iodine with a high EA[46], no bubble effect is expected to be observed. However, for nitrobenzene with a low EA[47] bubble effects are believed to be of importance.

The o-Ps intensity in some binary mixtures of organic solvents is then shown. Here proton scavenging in the positron spur and electron trapping in hydrogen-bonded clusters are used to explain the observed o-Ps intensities. The o-Ps lifetimes in the binary mixtures are correlated to the lifetimes predicted by the models of Levay and Hautojärvi, and Levay, Hautojärvi and Vertes. The inhibition caused by CS_2 in different alkanes and TMS is correlated to the energy, V_o, of the electron in the alkanes.

Finally a series of measurements on electron acceptors and CT-complexes in different solvents is presented. Here the o-Ps lifetime is used in order to obtain the CT-complexity constant. By use of the spur reaction model the intensity of the long-lived component is used to obtain information on the electron trapping probability and mechanism of electron reactions with acceptors in different solvents.

The bubble radii of the Ps bubble in the different organic solvents are shown in table 7.1. Notice the decrease in bubble radii from pentane to heptane. This decrease is obtained irrespective of whether the radii are calculated by use of the surface tension σ, or the FWHMs. With the exception of the CS_2 results, the average value of $\langle r_b/R_b \rangle = 1.293$, yielding a maximum deviation from the average of 3.3%. The maximum deviation from the average of the bubble radii (r_b) is 7.0%.

Table 7.1

The bubble radii R_b calculated by use of the FWHM (Γ_m) of the narrow component in the angular correlation distribution. R_b is obtained from Γ_m by use of formulae (5.56), (5.57), and (5.59). The bubble radii r_b are calculated by use of the surface tension σ of the liquids using formulae (5.48)

	Γ_m(mrad)	Γ_θ(mrad)	R_b(Å)	r_b(Å)	σ(dyn/cm)	r_b/R_b
n-pentane	2.53	2.25	4.70	6.22	16.0	1.32
n-hexane	2.54	2.26	4.68	6.00	18.42	1.28
n-heptane	2.60	2.33	4.54	5.86	20.31	1.29
benzene	2.80	2.55	4.15	5.37	28.88	1.29
o-xylene	2.75	2.49	4.25	5.31	30.10	1.25
CS_2	2.45	2.18	4.89	5.22	32.3	1.06
diethylether	2.57	2.30	4.60	6.13	16.96	1.33
TMS	2.53	2.25	4.70			

The rate constants between o-Ps and iodine, and o-Ps and nitrobenzene are presented in table 7.2.

Table 7.2

The bubble shrinkage velocity (v_s) in the different alkanes plus the rate constant (k) between iodine and o-Ps, and between nitrobenzene and o-Ps in the different alkanes. For weak electron acceptors (e.g. nitrobenzene), high v_s should according to the bubble shrinkage model result in low rate constants. For strong electron acceptors the rate constant should be independent of v_s

	σ(dyn/cm)	η(g/cm s)	$v_s = \frac{\sigma}{2\eta}$ (Å/ps)	k for I_2 (10^{10} M^{-1} s^{-1})	k for nitrobenzene (10^{10} M^{-1} s^{-1})
n-pentane	16.0	0.00227	0.352	10.1 ± 1	0.037 ± 0.003
n-heptane	20.31	0.004163	0.244	6.3 ± 0.5	0.31 ± 0.03
n-dodecane	25.42	0.0149	0.085	2.9 ± 0.3	1.1 ± 0.1

For iodine with an EA of 1.8 eV no bubble effects are expected and k decreases in going from pentane to dodecane. For nitrobenzene with an EA of 0.5 eV, bubble effects are expected and k increases in going from pentane to dodecane. Both for iodine and nitrobenzene in the alkanes, the intensity of the long-lived component decreases as the concentration of the two compounds increases. It was not possible to reasonably fit the intensities of the long lifetime to (5.99) so no inhibition cross sections are presented. Tao measured rate constants between o-Ps and iodine in alkanes[48]. In the same paper he also presents inhibition cross sections for iodine in alkanes. The rate constants determined by Tao were practically identical to the rate constants determined here, whereas his intensities of the long-lived component were rather different from the intensities determined in this work.

The following results concern binary mixtures of organic solvents. Here proton scavenging in the positron spur is expected to enhance Ps formation due to inhibition of electron-proton recombination.

The measured long lifetime intensities for the proton-scavenging cases are shown in fig. 16. In the dioxane-n-heptane mixtures the Ps yield

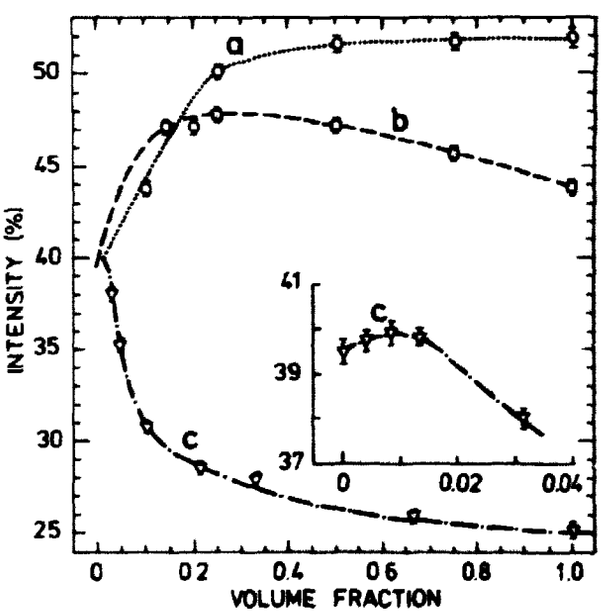

Fig. 16. The intensities of the long-lived component versus the volume fraction of a) dioxane in n-heptane (o), b) triethylamine in n-heptane (□), and c) pyrrolidine in n-heptane (▽). The curves are the best fit to the experimental points.

increases with increasing amounts of dioxane and is almost constant for dioxane concentrations higher than 25 vol. %. Also in the TEA-n-heptane mixture the Ps yield increases with increasing amounts of TEA until 25 vol. %. At higher concentrations, the intensity decreases to the intensity in pure TEA. For the pyrrolidine-n-heptane mixture, the Ps yield increases for increasing pyrrolidine concentration, but already from 1 vol. % pyrrolidine the intensity decreases rapidly towards the yield in pyrrolidine.

The o-Ps lifetimes calculated using the model no. (5. 91 a) are shown on fig. 17.

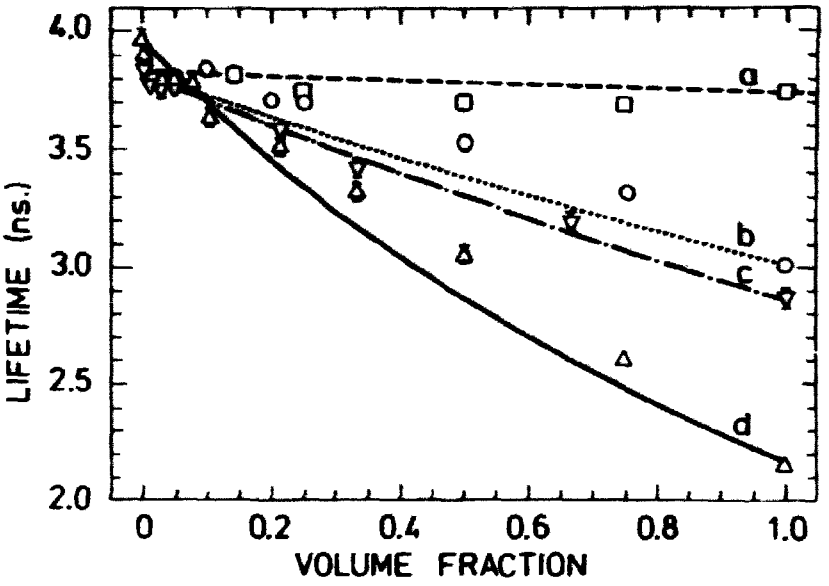

Fig. 17. The lifetime of the long-lived component versus the volume fraction of a) triethylamine in n-heptane (□), b) dioxane in n-heptane (○), c) pyrrolidine in n-heptane (▽), and d) carbondisulphide in n-hexane (△). The curves show the lifetimes calculated by use of model (5. 91 a) in the text and the lifetimes in the pure liquids.

Since the surface tension of the mixtures was unknown, no comparison was possible between the measured lifetimes and the model proposed by Tao (5. 92). Of the models in refs. 27 and 28, no. (5. 91) fitted the measured lifetimes better than no. (5. 90). In the pyrrolidine-n-heptane mixtures the fit was good for both models (5. 90) and (5. 91), for the CS_2-n-hexane and dioxane-n-heptane mixtures model (5. 91) was best, and for the TEA-n-heptane mixtures the two models gave practically the same results.

The shortest lifetimes, the median lifetimes, and their respective relative intensities are not presented. When three or more lifetimes are present in the spectrum, it is, in our experience, often difficult to obtain reliable absolute values for the two shortest lifetimes and their intensities. The unreliability of the shortest lifetimes is even more pronounced when large source corrections involving short lifetimes are to be performed. The problems involved in this are discussed in some detail in 37).

The results for CS_2 in the alkanes and TMS are shown on fig. 18.

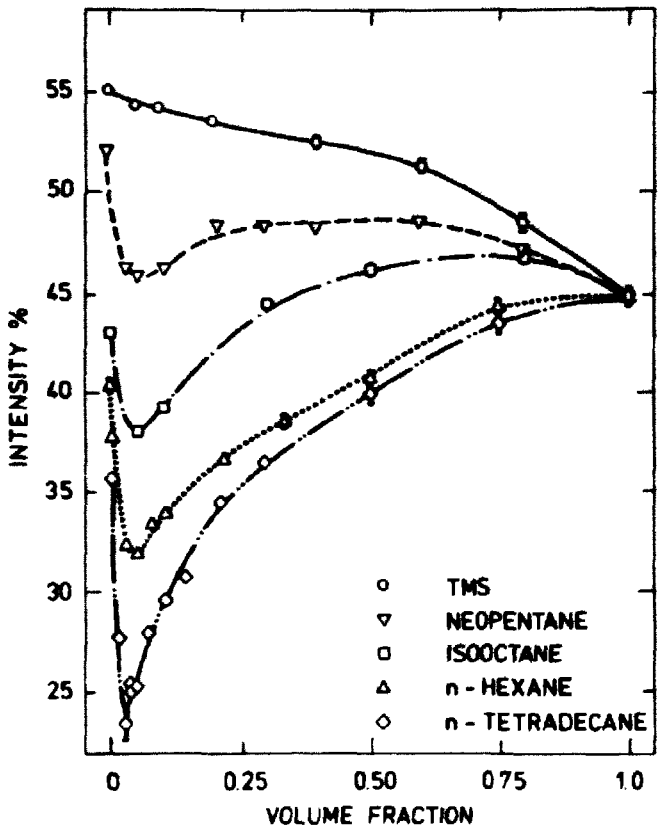

Fig. 18. The intensities of the long-lived component versus the volume fraction of CS_2 in various alkanes and TMS. The curves are drawn to give a best visual fit to the experimental points.

The energy difference between the electron in vacuum and the electron in the liquid is presented in table 7.3

Table 7.3

V_o for different alkanes and TMS. V_o is the energy difference between an electron in vacuum and the electron in the solvent. Negative V_o means energy is gained in bringing the electron from vacuum into the solvent[51]

	n-tetradecane	n-hexane	isooctane	neopentane	TMS
V_o (eV)	0.21[49]	0[50]	- 0.26[50]	- 0.38[49]	- 0.51[50]

where negative V_o means that energy is gained in bringing the electron from vacuum into the liquid. In vacuum, CS_2 has an EA of 0.98 eV[52]. When CS_2 is in a liquid in which it is a deep electron trap (n-tetradecane) the minima in the o-Ps yield are deep and narrow. In a liquid where the CS_2 trap is less deep (neopentane), the minima in the Ps yield are less deep and less well defined. No minima are observed in TMS.

For the other electron acceptors the long o-Ps lifetimes, or their inverse, the decay rates, are shown in figs. 19-21, 26, 28, 29 for the

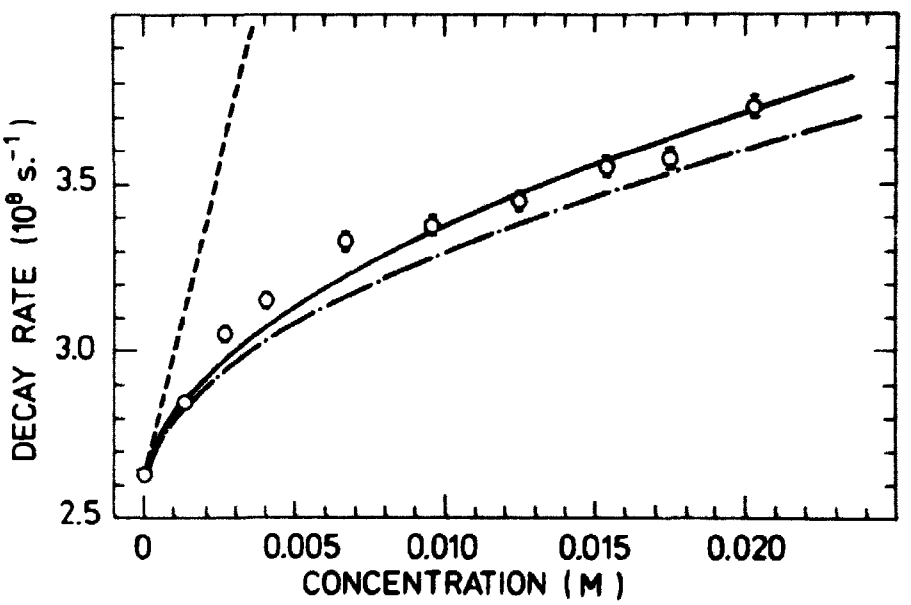

Fig. 19. The decay rate of the long-lived component versus the concentration of SO_2 for 1:1 SO_2:TMA in n-heptane. The dashed line corresponds to the decay rate if all the SO_2 was free (complexity constant K = 0 M^{-1}). The full line corresponds to K = 2000 M^{-1} and the dashed-dotted line corresponds to K = 2550 M^{-1}.

various solutions. Only the lifetimes for SO_2 in dioxane and n-heptane, and for TCNQ in tetrahydrofurane (THF), are not shown since they follow the relation (5.97) (with (AD) = 0) very closely, quite like the other case where no complex is present (TCNE in dioxane, fig. 21). The quenching constants (k), and λ_p, were determined for each set of measurements with only acceptor present by a least squares fit of eq. (5.87) to the measured lifetimes. The values are given in tables 7.2 and 7.4. The lifetime results of

Table 7.4

Main parameters extracted from the measurements. The upper values of σ or σ_1 are for τ_m = 0.3 ns, the lower ones in parentheses are for τ_m = 0.5 ns. The uncertainties on τ_p and I_o were estimated by computer, while those on k, k_1, σ, and σ_1 are visual estimates. The parameters in the table (for τ_m = 0.3 ns) were used in eqs. (5.87) and (5.99) to draw the curves in figs. 19-23 and 25, 26. Different I_o values for dioxane and n-heptane are results of different positron absorption in different sources.

Solution	k or k_1 (10^{10} M^{-1} s^{-1})	σ or σ_1 (M^{-1})	τ_p (10^{-9} s)	I_o (%)	K (M^{-1})
SO_2 in dioxane	1.5 ± 0.1	5 - 40 (10 - 70)	2.99 ± .02	32.7 ± .2	-
SO_2 in n-heptane	3.7 ± 0.2	0 (17 ± 3)	3.80 ± .03	32.2 ± .4	-
SO_2-TMA in n-heptane	small	15 ± 3 (15 ± 3)	3.80 ± .03	32.2 ± .4	2000
TCNQ in THF	3.4 ± 0.2	20 ± 5 (35 ± 5)	3.03 ± .03	16.9 ± .2	-
TCNQ-HMB in THF	small	150 ± 50 (150 ± 50)	3.03 ± .03	16.9 ± .2	1.5
TCNE in dioxane	1.6 ± 0.1	20 ± 3 (27 ± 3)	2.99 ± .02	38.6 ± .8	-
TCNE-HMB in dioxane	small	-	2.99 ± .02	38.6 ± .8	~0
PPS in water	0.006 ± 0.001	5.85 ± .1 (5.85 ± .1)	1.83 ± .03	20.8 ± .5	-
O_2 in n-heptane	0.74 ± 0.09		3.80 ± 0.03	40.7 ± .3	-

measurements on solutions also containing CT complexes were likewise analyzed by a least squares fitting of eq. (5.97) with [A] and [AD] from eqs. (5.96) and (5.95). k was known from pure acceptor solutions and k_1 and K were fitting parameters. It appeared that both for TCNQ-HMB and SO_2-TMA the best fit was obtained for very small K and k_1 large and negative. This, however, is unphysical unless one claims that the pick-off annihilation rate from the complex molecules is much less than that from the solvent, and that the comples replaces an unreasonable amount of solvent molecules. A value of k_1 in the order of 10^7-10^8 M^{-1} sec^{-1} or less would not be detectable since it would be too close to that of the solvent. So for the sake of simplicity k_1 was set equal to zero and K was determined to give the best visual fit of eq. (5.97) to the data. The values obtained in this way for K are shown in table 7.4, and they were used for the full curves in figs. 19 and 20. In fig. 19 the dashed-dotted curve shows the expected results for K = 2550 M^{-1} as determined optically[53]. It compares reasonably with our results of K = 2000 M^{-1}. For TCNQ-HMB in THF, we optically determined K to be 3.8 M^{-1}. The optical spectra, however, were unstable, probably because the oxygen dissolved in the THF took part in a decomposition of TCNQ. The lifetime results, obtained on degassed samples, gave reproducible results and K = 1.5 M^{-1} (fig. 20).

The rate constants for the free acceptors in the solvents with donor properties (THF and dioxane) are probably higher than noted in table 7.4, since in these solutions a certain fraction of the acceptors is bound to the solvent molecules. In this bound state the acceptor probably has a smaller reactivity, since the addition of electron donors to the solutions and the formation of CT complexes increases the o-Ps lifetime.

Quenching by PPS in water (fig. 26, table 7.4) is so weak that it may be ascribed to changes in the liquid structure at high PPS concentrations.

The results obtained for the relative intensity of the long-lived component for the various solutions are shown in figs. 21-27. It was possible to fit the concentration dependence of the relative intensity for all solutions by eq. (5.99), except for SO_2 in dioxane (fig. 24), oxygen in n-heptane (fig. 27) and maybe TCNQ-HMB in THF (fig. 25). In each case the procedure was first to determine σ from the results for solutions with only an acceptor present ((AD) = 0 in eq. (5.99)). For the equivalent solution additionally containing CT complex this value of σ was used in eq. (5.99) and σ_1 determined.

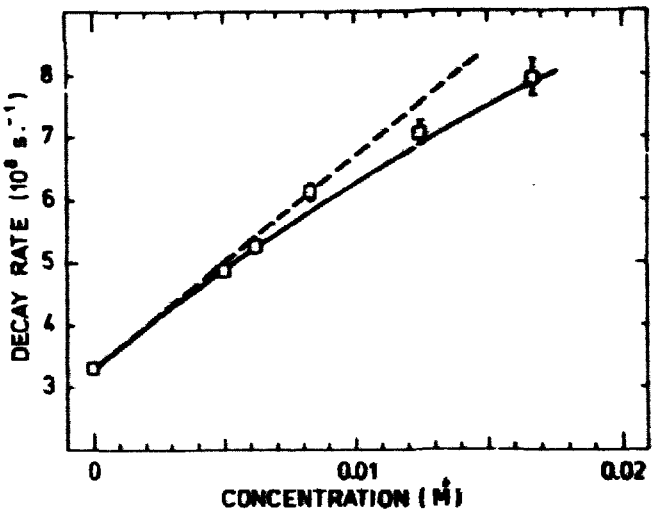

Fig. 20. The decay rate of the long-lived component versus the concentration of TCNQ for 1:10 TCNQ:HMB in THF. The dashed line corresponds to the complexity constant K = 0 M^{-1} and the full line corresponds to K = 1.5 M^{-1}.

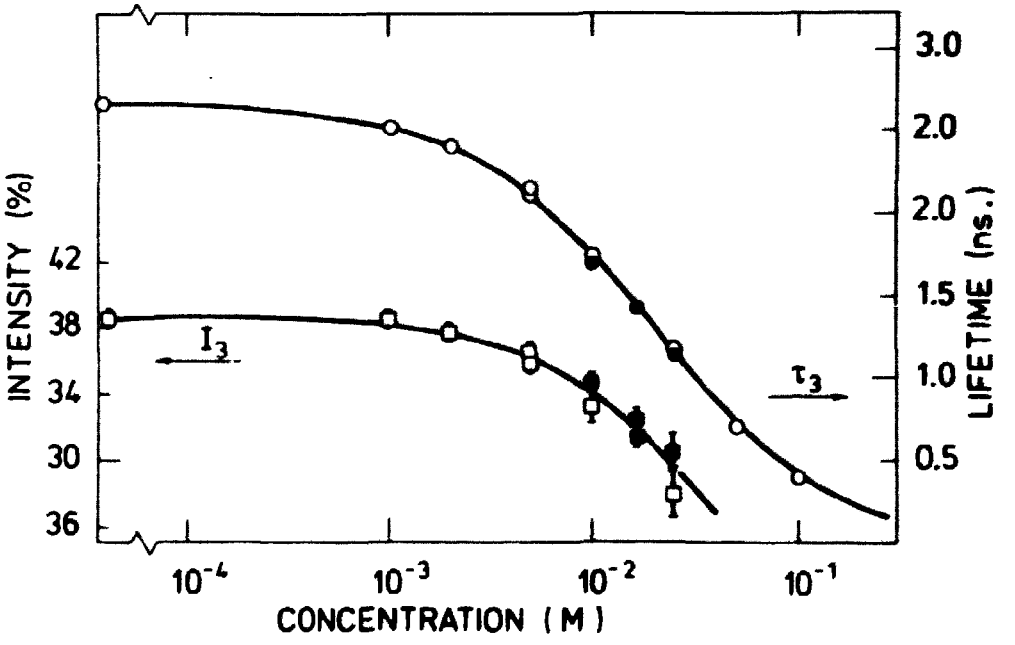

Fig. 21. The intensity (squares), and the lifetime (circles) of the long-lived component versus the concentration of TCNE in dioxane (open squares and circles). Black squares and circles correspond to HMB added in a concentration 10 times that of TCNE. The curves are drawn in accordance with formulae (5.97) and (5.99) in the text and the constants in table 7.4.

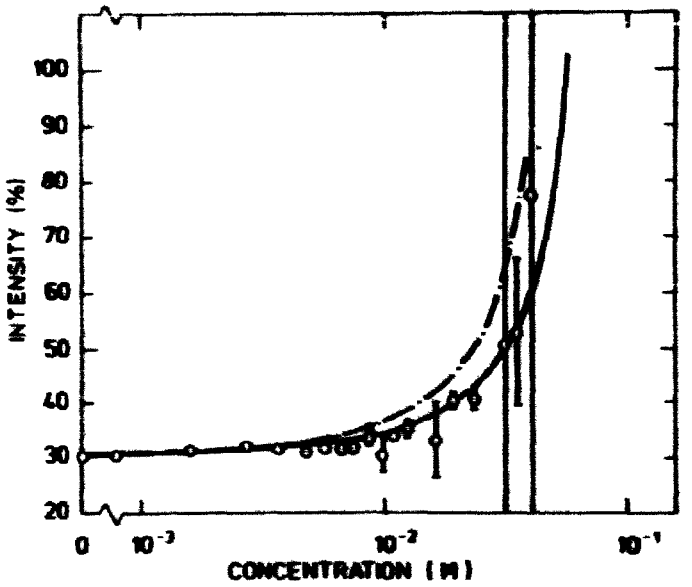

Fig. 22. The intensity of the long-lived component versus the concentration of SO_2 in n-heptane. The curves are drawn according to formula (5.99) and the constants in table 7.4. The dashed line corresponds to $\tau_m = 0.4$ ns, and the full line to $\tau_m = 0.3$ ns. Both curves are for $a = 0$ M^{-1}.

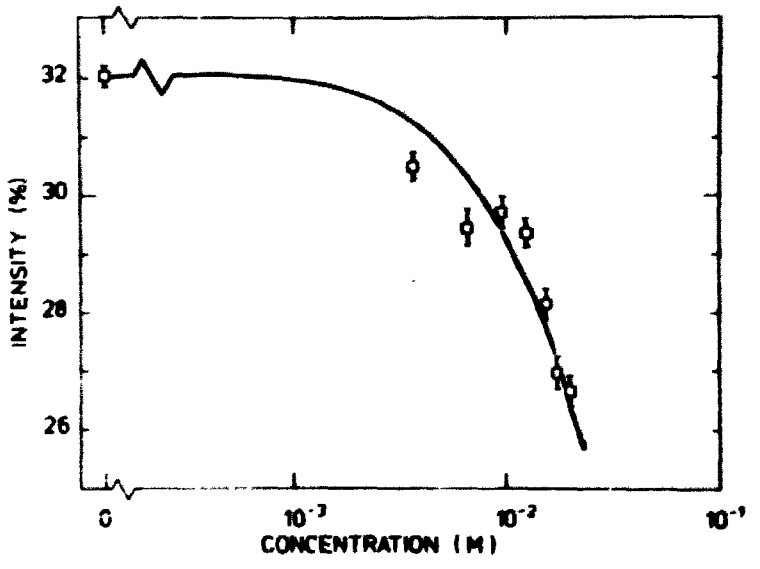

Fig. 23. The intensity of the long-lived component versus the concentration of SO_2 for 1:1 SO_2:TMA in n-heptane. The curve is drawn according to formula (5.99) and the constants in table 7.4.

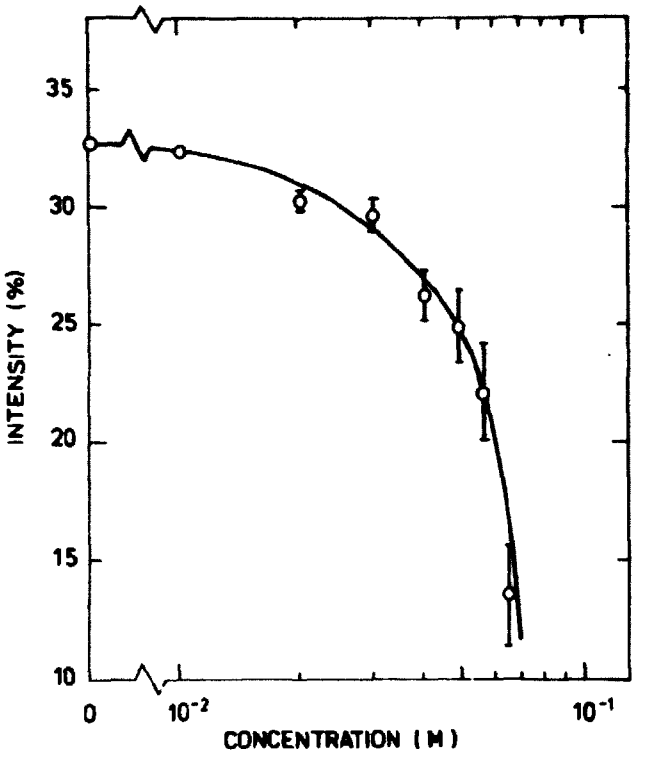

Fig. 24. The intensity of the long-lived component versus the concentration of SO_2 in dioxane. The curve is drawn to give the best visual fit and cannot be fitted according to formula (5.99).

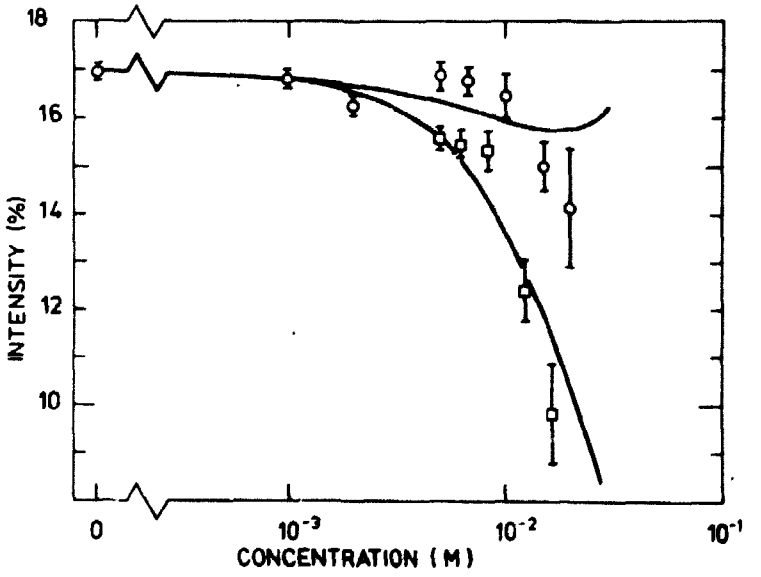

Fig. 25. The intensity of the long-lived component versus the concentration of TCNQ in THF (circles). Squares correspond to the same curve but with HMB present in a concentration 10 times that of TCNQ. The curves are drawn according to formula (5.99) and the constants in table 7.4.

The value of λ_c was calculated from eq. (5.87) and the long lifetime. The lifetime in the Ps-acceptor bound state, λ_m^{-1}, is expected to be in the region of 0.3-0.5 ns, and to estimate its influence on the results, σ and σ_1 were determined for both λ_m^{-1} = 0.3 and 0.5 ns. The values given in table 7.4 are those which gave the best visual fits of eq. (5.99) to the data. The upper ones are for λ_m^{-1} = 0.3 nsec, and the lower ones in brackets for λ_m^{-1} = 0.5 nsec. The full curves in figs. 21-23 and 25-26 were drawn from eq. (5.99) with the parameters for λ_m^{-1} = 0.3 nsec. While the σ's are rather sensitive to λ_m, the σ_1's for CT complexes are not, as seen in table 7.4. To fit the results for SO_2 in dioxane (fig. 24) to eq. (5.99), σ had to vary from 5 to 40 M^{-1} (λ_m^{-1} = 0.3 nsec), or from 10 to 70 M^{-1} (λ_m^{-1} = 0.5 nsec), as indicated in table 7.4. Hence, although the simple expression for the Ps yield fits the data very well in some cases (fig. 26), it completely fails to do so in others (fig. 24).

With O_2 in n-heptane as an exception, the relative intensity of the long-lived component in pure solvents, I_o (table 7.4), is not that of o-Ps. This is because the lifetime spectra were not corrected for absorption of positrons in the Ni foils surrounding the source. These foils give rise to a short-lived (~0.2 nsec) component of intensity 20-35% (depending upon the source used). It should be mentioned that the same source was used for each set of measurements.

To determine the complexity constants by optical methods, data from absorption measurements were fitted by the least squares method to eq. (5.101), the complexity constant K and extinction coefficient ε and ε_1 being fitting parameters. The values for ε were checked by comparison with values measured on the pure acceptor in the solvent. For the TCNQ-HMB complex in THF, we obtained K = 3.8 M^{-1}. However, as mentioned above, this complex was unstable during the recording of the optical spectra, and the result must be regarded with some reservation. For TCNE-HMB in dioxane, K was very small, of the order of 10^{-3} - 10^{-2} M^{-1}. The absorption band appeared with a maximum at 520 nm. The maxima for the SO_2-dioxane and TCNE-dioxane CT bands were at 240 and 350 nm, respectively.

To further investigate some of the implications of the interpretation of positron lifetime results (see next section), negative ion mass spectra of SO_2 and the SO_2-TMA complex were recorded. When SO_2 alone was measured, a SO_2^- signal corresponding to ca. 0.4% of the total negative ion yield was observed. This signal can be ascribed to 60 ppm SO_3 which is known to form SO_2^- + O under these circumstances. However, when the SO_2-TMA complex was measured an SO_2^- yield corresponding to ca. 3% of the total negative ion yield was observed. Further work in this field is in progress in our laboratory.

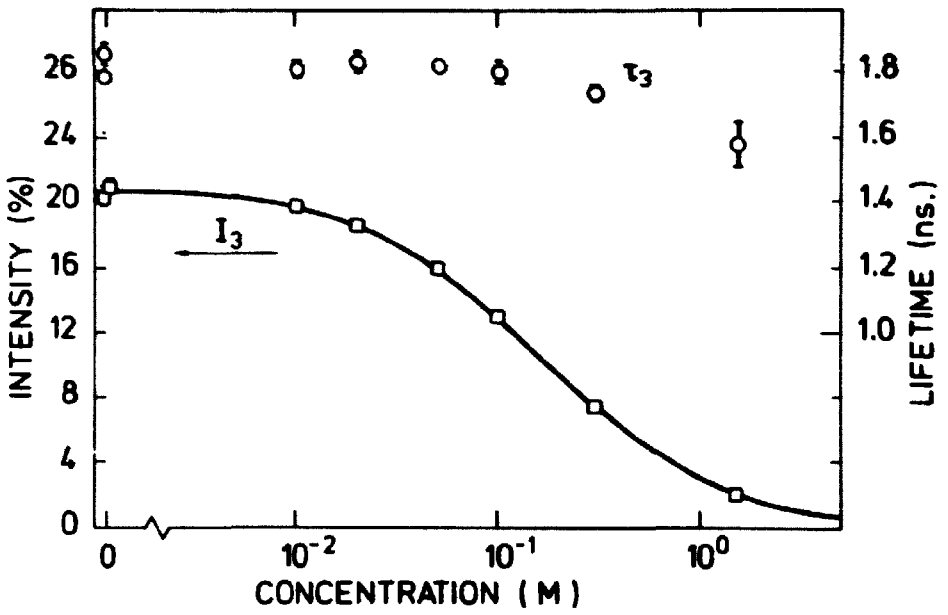

Fig. 26. The intensity (squares) and lifetime (circles) of the long-lived component versus the PPS concentration in water. The curve is drawn according to formula (5.99) and the constants in table 7.4.

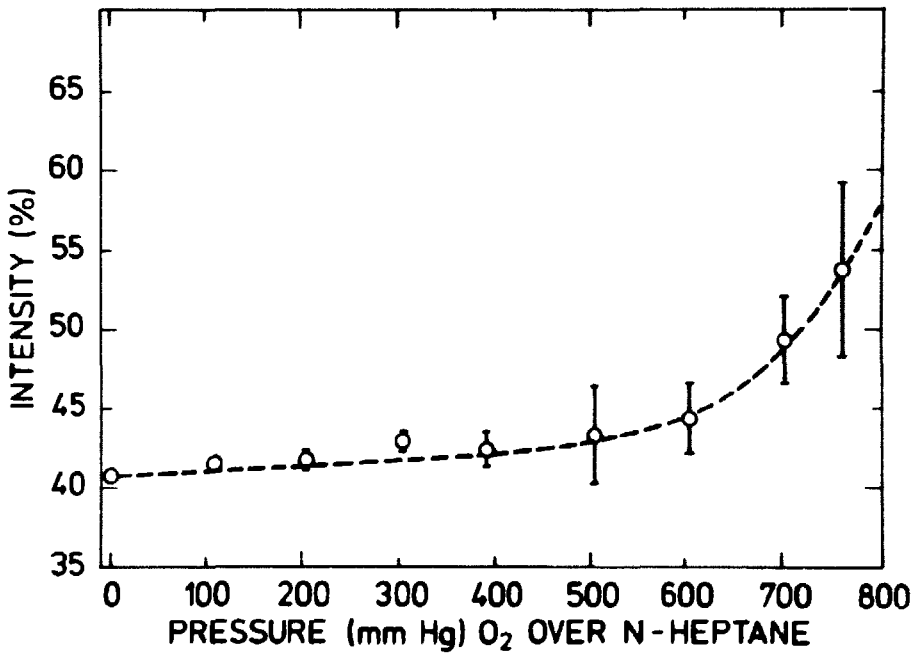

Fig. 27. The intensity of the long-lived component versus the oxygen pressure over n-heptane. For all the spectra, equilibrium between O_2 in n-heptane and O_2 above the n-heptane was established before the spectra were recorded. The intensities could not be fitted with (5.99) and the dashed curves are drawn to give a best visual fit.

8. DISCUSSION

It is, of course, incorrect to calculate Ps bubble radii by use of square well potentials with infinite high walls. Nevertheless the model can give some quantitative ideas about the sizes of the bubbles in which the Ps is trapped, assuming that Ps is trapped in a bubble. There are also several objections to using the narrowest component in a three Gaussian fit of the angular correlation curve as a measure of the momentum distribution of p-Ps in the liquid. There is no reason for a priori assuming that the p-Ps momentum distribution, as it is measured, can be well approximated with a single Gaussian.

With CS_2 as an exception, the intensity of the narrow component in the three Gaussian fit of the angular correlation curve was slightly more than one-third of the o-Ps intensity found from the lifetime measurements. For CS_2 the intensity of the narrow component (8.5%) was substantially less than one-third of the o-Ps intensity (44%) found from lifetime measurements. This indicates that the narrow component for the CS_2 does not represent the p-Ps momentum distribution in the same way as is the case for the other liquids presented.

If one assumes that the Ps is contained in a bubble in the liquids, the two methods mentioned for estimating the bubble radii seem reasonable. It is interesting that the average or effective bubble radii determined by the two methods do not differ significantly from each other.

In order to determine whether the bubble has any effect on the reactions between Ps and electron acceptors, Goldanskii et al. determined the rate constant between o-Ps and nitrobenzene in octanol as a function of temperature[54]. As the temperature increased from room temperature to 70-75°C, the reaction rate between nitrobenzene and o-Ps increased due increased mobility of the two components with increasing temperature. When the temperature was increased above 70-75°, the reaction rate decreased. This was explained as being due to the increased shrinking velocity $v_s = \frac{\sigma}{2\eta}$ of the Ps bubble as a result of changes of σ and η. At higher temperatures, the bubble shrank very fast and the time that the Ps spent in the complex decreased. These results indicate that Ps does form a complex with nitrobenzene. Ps oxidation could not explain the maximum in the reaction rate. It could, however, be argued that the decrease in the reaction rate was not due to rapid bubble shrinkage but a result of decreased complexity constant with increased temperature.

Therefore another series of experiments was planned in order to evaluate whether bubble effects play any role for the reaction mechanism between o-Ps and electron acceptors. This time a strong acceptor (iodine) and a weak acceptor (nitrobenzene) were used in different alkanes all having the same temperature. The solvent effects on the complexity constant are assumed to be the same for both the iodine-Ps and the nitrobenzene-Ps complex. This means that if the complexity constants for the iodine-Ps complex decrease in going from pentane to heptane as solvent, the same effect is expected for the nitrobenzene-Ps complex. As shown on table 7.2, this is not the case. For the iodine-Ps reaction the effective rate constant decreased by a factor of 0.62 in going from pentane to heptane. For the nitrobenzene-Ps reaction the effective rate constant increases by a factor of 8.4 in going from pentane to heptane. This is just what should be expected according to the bubble reaction model.

According to the bubble model, the rate constant should really be a constant over a wide concentration range. From figs. 28 and 29 it can be seen that the rate constant for nitrobenzene-Ps, where bubble effects are important, seems at least as constant as the rate constant for iodine-Ps where no bubble effects are expected to be important. The much smaller rate constant between o-Ps and nitrobenzene, compared to the rate constant between iodine and o-Ps, can be explained as follows. When the o-Ps is in the heptane its pick-off annihilation rate is $2.8 \cdot 10^8$ sec^{-1}, when the o-Ps is trapped on an acceptor the annihilation rate goes up by a factor of ~ 10. When o-Ps is trapped on an iodine molecule (high EA) the Ps bubble shrinks. This shrinking does not affect the iodine-Ps complex. When the o-Ps is instead trapped on nitrobenzene (low EA), the bubble shrinking will cause a splitting up of the complex and the o-Ps will again be back in the solvent where it has a low annihilation rate. So when the acceptor is nitrobenzene the o-Ps will only spend a relatively short time in the complex, where the annihilation rate is high, and a comparatively longer time in the solvent, where the annihilation rate is low.

The bubble shrinking is also believed to influence the o-Ps-O_2 reaction in n-heptane, whereas the o-Ps-SO_2 reaction in n-heptane seems not to be influenced by the bubble shrinking.

The electron affinity of SO_2 is 1.097 eV[55]. The electron affinity of O_2 is 0.44 eV[56]. For SO_2 in n-heptane the intensities of the long lifetimes can be fitted by (5.99), whereas for O_2 in n-heptane the intensities of the long lifetime cannot be fitted with meaningful values by (5.99). This indicates that bubble effects play an important role for the reaction between O_2 and

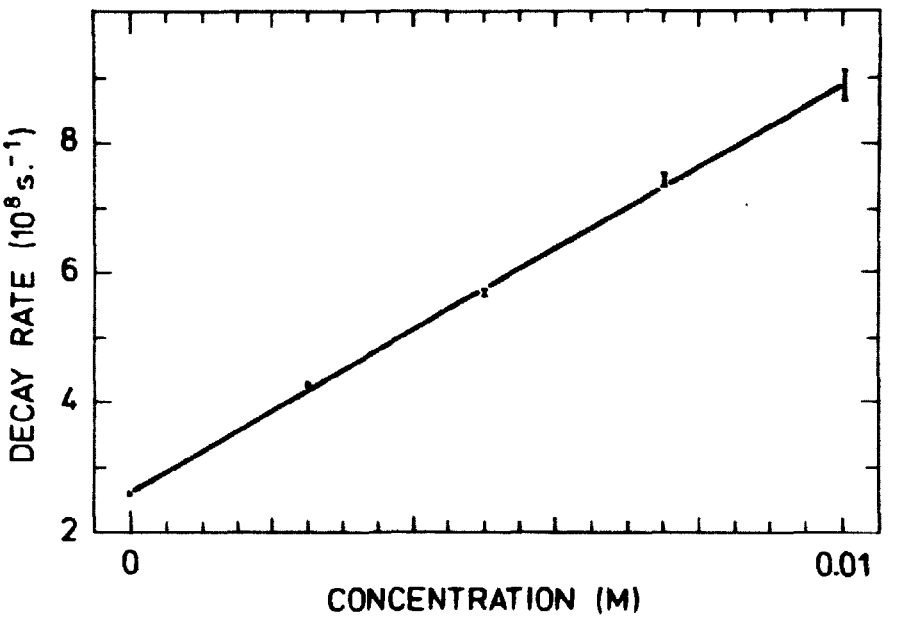

Fig. 28. The decay rate of o-Ps versus the concentration of iodine in n-heptane. The slope of the curve gives the effective rate constant.

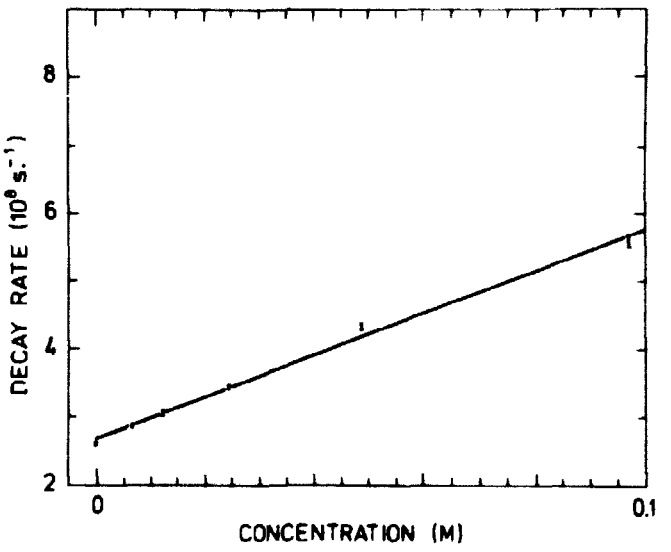

Fig. 29. The decay rate of o-Ps versus the concentration of nitrobenzene in n-heptane. The slope of the curve gives the effective rate constant.

o-Ps, whereas they seem to have no influence on the o-Ps-SO_2 reactions. The rate constants between o-Ps and O_2, SO_2, iodine and nitrobenzene in n-heptane are $0.74 \cdot 10^{10}$ M^{-1} s^{-1}, $3.7 \cdot 10^{10}$ M^{-1} s^{-1}, $6.3 \cdot 10^{10}$ M^{-1} s^{-1} and $0.31 \cdot 10^{10}$ M^{-1} s^{-1} respectively. The rather low reaction constant for O_2 compared to SO_2 and iodine indicates again that bubble effects are of importance for oxygen quenching, just as it is observed for the quenching of o-Ps by nitrobenzene.

Next some spur processes for binary mixtures of dioxane, TEA and pyrrolidine in n-heptane are discussed on the background of the spur reaction model. From the spur reaction model it is predicted that the addition of proton scavengers to alkanes should enhance the Ps yield due to reduced electron-proton recombination and consequently more free electrons for Ps formation. Here only spur processes of importance for the interpretation of our data will be discussed in detail. The spur processes that are believed to be responsible for Ps formation have not been thoroughly investigated yet. Hence, only a qualitative or semiquantitative discussion of the data can be given.

When a positron is stopped in n-heptane the most important primary ionization products are expected to be similar to those produced by the stopping of epithermal electrons by hydrocarbons

$$e^+ + C_7H_{16} \rightarrow C_7H_{15}^+ + H^+ + e^+ + 2e^- . \qquad (8.1)$$

In the presence of molecules with high proton affinity (PA), such as ammonia (PA = 9.5 eV), the following reactions can occur[57,58]:

$$H^+ + NH_3 \rightarrow NH_4^+ \qquad (8.2)$$

$$C_7H_{15}^+ + NH_3 \rightarrow C_7H_{14} + NH_4^+ . \qquad (8.3)$$

Reactions (8.2) and (8.3) will compete with e^-, H^+ and e^-, $C_7H_{15}^+$ recombinations, thereby making more free electrons available for Ps formation. This means that when molecules with high PA are added to alkanes, the Ps yield will increase unless other processes interfere.

The first molecule for which this reaction was found was dioxane. The proton affinity of dioxane will be close to that of C_2H_5OH[59], which is 8.4 eV. For water, the PA is 7.3 eV[59]. Hence, replacing R_1 and R_2 in R_1-O-R_2 from hydrogen by a more electron-donating group, such as CH_2-CH_2, seems to increase the PA.

As the dioxane concentration increases the amount of free H^+ and $C_7H_{15}^+$ will decrease. Consequently the electron concentration will increase, and the yield of Ps will increase. Since dioxane predominantly exists in its trans form with no dipole but only a quadrupole moment, its electron or positron solvating properties are belived to be small.

Another molecule with a high PA but with a dipole moment different from zero is TEA. TEA will have a PA close to that of trimethylamine, which is 9.2 eV[60]. Hence, also TEA is expected to increase the Ps yield owing to scavenging of H^+ in the positron spur. This increase in the Ps yield was observed for concentrations of TEA in n-heptane up to 25 vol. %. As shown in fig. 16 the Ps yield decreases for TEA concentrations higher than 25 vol. %. The explanation of this is believed to be found in the electron- and positron-solvating properties of TEA due to its polar structure (see below).

Pyrrolidine is another molecule with a high PA and a dipole moment different from zero. The PA for pyrrolidine will be close to 9.3 eV, as it is for piperidine[60]. In addition, pyrrolidine contains an NH group which enables it to form hydrogen-bonded clusters similar to those formed by alcohols in alkanes[61].

The increase in Ps yield resulting from adding small amounts of pyrroline to the n-heptane is believed to be due to proton scavenging. At pyrrolidine concentrations higher than 1 vol. %, pyrrolidine is believed to form clusters which trap electrons to such an extent that the Ps yield decreases.

Measurements performed by Kemp et al.[62] indicate that such clusters do trap electrons. Beck and Thomas[63] have shown that adding ethanol to n-hexane decreases the mobility of the electrons greatly. The authors have suggested that this decrease in mobility is due to trapping of electrons in alcohol clusters. Recently Brandon and Firestone[64] measured the optical spectrum of electrons solvated in ethanol clusters in various alkanes. The spectrum appears for ethanol concentrations of 1-2 mol%. This agrees very well with the pyrrolidine concentration at which the Ps yield in the pyrrolidine n-heptane mixture starts to decrease. In the same article (64) it is also shown that amines (ethylenediamine) solvate electrons.

Hence, we expect the Ps yield to decrease on account of electron and positron trapping in the pyrrolidine clusters. The mobilities of the electrons and the positron are greatly decreased on trapping. Also the Coulomb forces are decreased owing to dielectric shielding. Hence, the electron-positive ion recombination processes and the out-diffusion of the particles from the spur will increase in importance compared with Ps formation, i. e. the Ps yield will decrease. This is in agreement with the fact that the Ps

yield is roughly a factor of two lower in water and alcohols than it is in hydrocarbons. In ref. 27 dioxane-water mixtures were investigated. The intensity of o-Ps decreased rapidly when water was added to dioxane. Only 10% of water decreased the Ps yield down to about its value in water. Roughly this value was also found at higher concentrations. This result is very similar to the pyrrolidine results above 1 vol.%, and is interpreted in the same way as being due to the effect of trapping of the electrons and the positron in water clusters in dioxane.

It is not yet known whether Ps formation in polar liquids occurs with a) mainly unsolvated (dry) electrons, b) mainly solvated electrons, or c) with both unsolvated and solvated electrons. Obviously, this depends on whether the Ps formation time is a) shorter than, b) longer than, or c) comparable with the electron solvation time. It must be realized that the solvation time measured by light absorption[65-66] need not be the time which is of importance for Ps formation, where even a small degree of electron localization seems to influence the Ps yield. These problems have recently been discussed by Byakov et al.[67]. Recent experiments indicate strongly (ref. 37) that at least in water the Ps is mainly formed with dry electrons. Fast spur reactions with dry- and solvated electrons are discussed in some detail in refs. 68 and 69.

The great differences in particle solvation influence on the Ps yield when the solute is changed from dioxane (only quadrupole moment) to TEA (dipole moment) and further to pyrrolidine and water (dipole moments and hydrogen bonds) show that Ps formation measurements may give useful information on the properties (clustering, etc.) of liquid mixtures.

The binary mixtures of alkanes, TMS and CS_2 differ in many respects from the binary mixtures just mentioned.

By use of pulse radiolysis, Simonsen[70] found that CS_2 traps free electrons in n-hexane. The assumed CS_2^- ions, or perhaps the $C_2S_4^-$ ions, are correlated to an absorption band at 257 nm. Owing to the strong absorption from the free CS_2 at this wavelength it has not been possible to see the line from CS_2^- at higher concentrations than 5 vol.% CS_2 in n-hexane.

According to the spur model, trapping of electrons normally causes a decrease in the Ps yield. This was also observed and is shown on fig. 18, but at CS_2 concentrations higher than 5 vol.% the Ps yield increases. With increased $[CS_2]$ the average distance between two CS_2 molecules decreases. This means that the tunelling probability between two neighbouring CS_2 molecules increases, and the result of this will be an increase in the electron mobility.

As mentioned in ref. 10, liquids with the highest electron mobilities (e.g. neopentane and other more spherical hydrocarbons) give higher Ps yields than liquids with lower electron mobilities (e.g. n-pentane and linear hydrocarbons). We therefore expect the Ps yield to increase again as shown in fig. 18. Generally speaking, a rather localized, slowly moving electron seems to be less effective in forming Ps with the positron, in competition with other processes, than a more delocalized, faster moving electron, at least for electron mobilities that are typical of hydrocarbons. Of course, the positron can pick off the electron from CS_2 as its electron affinity is 6.8 eV compared with 0.98 eV for CS_2. As mentioned in ref. 1, the mobility of free electrons the first few ps after their creation is expected to be rather high in pure CS_2. This mobility does not seem to have been measured yet.

When n-hexane is exchanged with a solvent with higher V_0 the trap on the CS_2 molecules becomes deeper. This could mean a higher trapping probability and a deeper minima in the Ps yield, as observed. If liquids with lower V_0 than that of n-hexane are used, the CS_2 trap is lees deep. This would mean lower trapping probability and the minima in the Ps yield could be less deep and less well defined, as observed of neopentane and isooctane (see fig. 18). If, e.g., TMS with a very low V_0 is used, it seems that the CS_2 trap is so shallow that it is unable to trap electrons, and no minima is observed in the Ps yield as more and more CS_2 is added to the TMS solution. For the moment it is not possible for the author to explain the maxima on the neopentane-CS_2- and isooctane-CS_2 curve.

A minimum in the Ps yield, similar to that shown in fig. 18, was found at around 50% mixing ratio for mixtures of acetic acid and acetone by Goldanskii et al.[71] in a mixture of acetic acid and acetone. These authors explain their results in terms of the Ore gap model. Curves which exhibit minima, as well as curves exhibiting maxima, can easily be obtained in terms of the Ore gap model. In binary mixtures a certain curve can be obtained by choosing suitable values for the cross sections for inelastic scattering of positrons on one type of molecule in the Ore gap of the other type of molecule.

From the point of view of the spur model this system is rather complicated. The spur electrons add to the acetone molecules as in the CS_2 case, they react with the acetic acid molecules, and less strongly with the acetate ions[30, 72]. Further the negative acetone ions can be protonated by acetic acid molecules, similar to the protonation by the water molecules[30]. The liquids are polar and hence solvation is also of importance. Apparently it is difficult within the presently available knowledge of spurs to interpret these data unambiguously in terms of the spur reaction model.

Finally, we shall discuss the reactions between electrons, Ps and electron acceptors.

Since Ps has a very low ionization potential (6.8 eV), it is expected to be a good electron donor that will react with an electron acceptor to form a CT complex. When o-Ps is in such a complex the electron density at the position of the positron intensifies and the annihilation rate increases [17].

We have observed this quenching of o-Ps (figs. 19, 20, 21, 26 and table 7.4). It is also to be expected that if an electron acceptor is already taking part in CT complexes, its ability to form a complex with Ps will be strongly reduced. This explains why CT complexes do not seem to quench o-Ps to any significant extent (table 7.4).

Normally, the Ps lifetime is decreased when Ps reacts with an electron acceptor (Ps quenching), and also the Ps yield seems to decrease as the acceptor concentration increases [73, 54]. If the electron affinities (EA) given in refs. 47, 52 are correct, the Ps quenching ability is not solely dependent on the EA of the acceptor and the properties of the solvent [1]. For instance, CS_2 with an EA of 0.98 eV [52] shows hardly any quenching properties [2], whereas nitrobenzene with an EA of 0.5 eV [47] exhibits typical quenching properties [54].

According to the spur reaction model, electron acceptors should inhibit Ps formation as a result of electron scavenging in the positron spur. The parameters which determine whether an acceptor can attach an electron within a time relevant for Ps formation are therefore important and will be discussed in some detail below.

When a low energy electron collides with an acceptor molecule, different processes can occur [74, 75, 76, 77].

$$A + e^- \rightarrow A^{*-} \begin{cases} \rightarrow A + e^- & (8.4a) \\ \rightarrow C + B^- & (8.4b) \\ \rightarrow A^- & (8.4c) \end{cases}$$

These processes are mainly studied as gas phase reactions. However, most of the arguments can be modified in order to apply to liquid phase reactions too. In which case, of course, the EA and dissociation energies must be corrected for solvent effects.

Which of the processes (a), (b) or (c) will take place depends on the energy of the electrons, the number of degrees of freedom in the acceptor, and the medium in which the process takes place. For small molecules with few degrees of freedom and weak or no interaction with the medium, and for electrons with energies from thermal and up to the appearance

potential AP of one of the fragments (e.g. B^-), process (a) will be most probable (see arguments for O_2 and SO_2 later in this section). (The AP for B^- is the lowest electron energy for which B^- is created). For such small molecules (A), a typical lifetime of A^{*-} is 10^{-15} s [77], but it can be much longer. The time for radiative relaxation to the ground state is $\sim 10^{-8}$ s, so the probability that the electron stays on the molecule is $\sim 10^{-7}$. Another type of relaxation is through collision with other molecules. A typical collision frequency in liquids is 10^{13} s^{-1}. So within 10^{-13} s the molecule is expected to relax to the ground state through collisions. Nonetheless the probability that the electron will stay on the acceptor is $\sim 10^{-2}$. Hence, contrary to what one might expect at first sight, i.e. that an acceptor in a liquid always interacts with the solvent molecules to such an extent that it can attach an electron, this seems only valid to a limited extent.

For electrons with energies in the interval $AP \leq E \leq AP + 1$ eV, a highly probable process is the breaking of a bond:

$$A + e^- \rightarrow B^- + C.$$

In this case the electron-accepting capacity of the acceptor will be high. For molecules such as Cl_2, Br_2, and N_2O, where the EA of the molecule is higher than or equal to the dissociation energy of a bond in the negative ion, this process will occur for electrons with thermal or higher energies [78]. The excess energy can be removed by the fragments as kinetic energy.

Process (8.4c) is most probable for large acceptor molecules. Here the molecule can relax electronically by distributing the energy gained by attaching the electron among its vibrational degrees of freedom. This is, for instance, the case for molecules such as SF_6 and nitrobenzene. The negative ion for such molecules will appear even for the lowest electron energies. Also this type of molecule will have an appreciable electron-accepting capacity.

Processes (8.4b) and (8.4c), where the electrons created in the spur will be trapped and localized, will inhibit Ps formation. Process (10a) will not inhibit Ps formation significantly if the lifetime of the A^{*-} is small compared to the Ps formation time $\sim 10^{-11}$ s. If the lifetime of A^{*-} is longer than $\sim 10^{-11}$ s, as it seems to be for CS_2^{*-} [7, 52, 79], also this process will inhibit Ps formation. What is important for Ps formation is the ability of the acceptors to trap and localize electrons for periods longer than $\sim 10^{-11}$ s. Acceptor reactions with the spur electrons taking place after a time typical for the Ps formation will have no practical influence on

the Ps formation. When Ps is formed as $e^+ + e^- \rightarrow$ Ps, the released energy can be removed by the molecules which are separated when Ps creates its bubble. Furthermore, the reaction between charged particles and electrons differs from the reactions between neutral molecules and electrons, as discussed briefly at the end of this section. With these considerations in mind we now proceed with a discussion of our experimental results.

For SO_2 in n-heptane we find σ equal to 0 and 17 M^{-1} for the extreme λ_m values, while σ_1 for the SO_2-TMA CT-complex is 15 M^{-1} in both cases. This tendency of the CT-complex to inhibit more strongly than the acceptor by itself is evident for TCNQ-HMB in THF. (The effect of the donor by itself is in all cases very small at the concentrations used). Using the SO_2-TMA complex as an example, we shall in the following interpret this result in the framework of the spur reaction model.

The weak inhibition (if any) by SO_2 in n-heptane is ascribed to the weak electron capture capacity of SO_2 in n-heptane. The n-heptane SO_2 interactions is rather weak and it seems as if SO_2 in n-heptane cannot get rid of the energy gained by attaching an electron to the SO_2, and therefore it scatters the electrons according to formula (8.4a). Hence SO_2 is a weak inhibitor. When TMA is added to the solution and the SO_2-TMA complex is formed, SO_2 can catch an electron and release the excess energy by breaking the SO_2-TMA bond in forming SO_2^- and TMA. This process follows (8.4b) and the interpretation of the reaction mechanism is supported by negative ion mass spectroscopy results (see section 7).

If n-heptane as solvent is substituted by a solvent with donor properties such as dioxane, SO_2 and the solvent will interact and form a CT complex. Again it is possible for SO_2 to get rid of the excess energy by breaking the SO_2 dioxane bond, and again we get inhibition as shown on fig. 24.

Goans and Christophoron[80] have shown that O_2 in N_2, C_2H_2 and C_2H_6 is able to attach low energy electrons and form O_2^-. This attachment has a maxima for electron energies of 0.04 eV and the attachment cross section practically disappears for electron energies of 0.15 eV. The attachment rate increases strongly as the carrier gas pressure increases. This shows that relaxation phenomena are of great importance for the attachment rate. Pure O_2 at low pressure ($\leq 10^{-5}$ mm Hg) is unable to form stable O_2^- [78]. By very reasonable assumptions, the autoionisation lifetime for O_2^{*-} has been estimated to be $\sim 2 \cdot 10^{-12}$ s [80].

Also SO_2 can attach low energy electrons and form SO_2^- via a nuclear-excited Feshbach resonance mechanism[81]. The attachment rate exibits a maxima for electron energies of 0.05 eV. Again the attachment cross section increases with increased carrier gas pressure showing that relaxation phenomena are of great importance for the attachment. The autoionisation lifetime for SO_2^{*-} is estimated to be $> 2 \cdot 10^{-10}$ s. The radiative stabilization rate of SO_2^{*-} is $\sim 1.8 \cdot 10^6$ s^{-1}. These results indicate that both SO_2 and O_2 in liquids should be able to inhibit Ps formation; at least if a major part of the Ps is formed with electrons of energies close to 0.04 - 0.05 eV. If, however, the major part of the Ps is formed with less energetic electrons or electrons with energies from .1-3 eV, it is reasonable that practically no inhibition is observed, anyhow it seems very unlikely that Ps should be formed with electrons with energies above 1 eV. For electrons with energies above 3 eV the attachment cross section for both O_2 and SO_2 increases due to dissociative attachment (8.4b). The question of whether or not O_2 and/or SO_2 inhibit Ps formation in the alkanes seems to be unanswered at present.

Finally, it can be mentioned that the autoionisation lifetime of excited negative ions decreases rapidly with increasing energy of the attached electrons[82]. For large electron acceptors ($M_W \gtrsim 100$), the autoionisation lifetime can be several hundred μs for electron energies $\sim$ 0.0 eV[83].

In the case of larger acceptors, such as TCNQ, one expects that process (8.4c) is possible and that the TCNQ alone can inhibit Ps formation. This expectation seems valid (fig. 25, table 7.4). However, the lone pair of the oxygen in THF has donor properties, so also here one may expect some CT complexes to be formed and the process

$$TCNQ\text{-}THF + e^- \rightarrow TCNQ^- + THF$$

to take place. Probably both processes take place. At all events the formation of the TCNQ-HMB complex strongly increases the inhibition (fig. 25, table 7.4). A 0.2 M solution of HMB in THF had practically the same lifetime spectrum as pure THF. This indicates that in liquids process (8.4a) is more efficient at electron scavenging than process (8.4c). TCNE in dioxane very much resembles TCNQ in THF, but the addition of HMB to the solutions had no effect on the lifetime spectra, as shown on fig. 21. Since the optical spectra indicate that very small amounts of TCNE-HMB are formed (section 7), it is reasonable to expect that the influence of the complex on the Ps lifetime spectra is negligible, just as is observed.

PPS is a salt and electron acceptor. In this twitterion the propane group can allow the $-SO_3^-$ group to approach the pyridine ring, and in this way form an intramolecular CT complex. PPS is a good electron acceptor as shown by Hickel[84], who determined its rate constant with hydrated electrons in water to be $(2.5 \pm 0.3)\ 10^{10}\ M^{-1}\ s^{-1}$. As a large solvated acceptor, PPS is expected to inhibit Ps formation, which is in fact the case, as seen on fig. 26. To the author's knowledge, this is the only example, together with NO_3^- in water, where the inhibition has been shown to follow the model of Green and Bell (eq. 5.100) (ref. 38) almost exactly.

The main effects of adding electron donors to solutions with acceptors were also observed by Hautojärvi and Levay[85]. When they added pyridine to a solution of iodine in cyclohexane, they observed an increase in the o-Ps lifetime and a stronger inhibition.

Since Ps formation takes place within the ps region[37], the interpretation given above of the inhibiting effect of CT complexes means that it may be difficult for an acceptor to get rid of excess energy within a few ps. However, also at longer times there may be difficulties in getting rid of excess energy.

Recent studies of electron neutral-molecule reactions in hydrocarbons[86-89] have shown that the rate constant is not proportional to the electron mobility in many cases. Hence the reactions are not diffusion-limited. On the other hand, the electron-ion recombination in the spurs of several liquids (including hydrocarbons) was well described by a diffusion-controlled-reaction theory. Hence, the attachment of electrons to neutral molecules is rather difficult, also at longer times after the creation of the spur. From our results we expect that the rate of an electron neutral-molecule reaction is strongly increased when the molecule takes part in a CT comples. Perhaps this effect will permit a study of diffusion-limited electron reactions with small neutral molecules (like SO_2) having reasonably small reaction radii.

9. CONCLUSION

There seems to be strong evidence that Ps is contained in a bubble in several organic liquids.

An argument in favour of this supposition is the change in the rate constant between o-Ps and iodine/nitrobenzene in the different alkanes. The change in the rate constant can easily be explained as the result of bubble shrinkage, but it is difficult to explain by other models. Also the

fact that the narrow component in the three Gaussian fit of the angular correlation curve is considerably broader than the resolution of the apparatus, speaks in favour of the existence of the bubble. Believing the p-Ps momentum distribution to be reasonably well represented by the narrow component leads to the conclusion that the p-Ps momentum corresponds to kinetical energies much larger than thermal. These high energies would be expected if the Ps was caught in a potential well (here the bubble).

This broadening of the narrow component can be used in calculating the radii of the bubbles where the Ps is caught (5.59). These bubble radii can apparently also be calculated from the surface tension of the liquids (5.48). The bubble radii calculated from the two methods mentioned are in reasonable agreement with each other.

The fact that the Ps is contained in a bubble in the liquids strongly influences the way in which the Ps reacts with electron acceptors. For electron acceptors with little EA, the lifetime of the acceptor-Ps complex will be reduced due to bubble shrinkage. The reduced complex lifetime will influence the effective o-Ps-acceptor rate constant in such a way that it seems much smaller than it would have been for strong acceptors. The more rapidly the bubble shrinks, the smaller will be the apparent rate constant.

In considering the probabilities of Ps formation, the three effects predicted by use of the spur reaction model of Ps formation[10] could be found. The addition of the three proton scavengers-dioxane, triethylamine, and pyrrolidine- to n-heptane increases the Ps formation. This is interpreted as being caused by scavenging in the positron spur of protons that would otherwise react with electrons. Hence, more electrons are available for Ps formation. Also the predicted minimum in Ps formation in the carbon disulphide-n-hexane mixtures was found. This minimum is interpreted as caused by trapping of electrons on carbon disulphide at a rather low carbon disulphide concentration, while tunnelling of electrons results in a higher electron mobility, and therefore a greater probability of Ps formation, at a high concentration of carbon disulphide. The effect of changing the V_o of the solvents with CS_2 also proved to be as predicted by the spur model. In a solvent with positive V_o, the CS_2 trap becomes deep, and the minima in the Ps yield become deep. For solvents with high negative V_o (TMS), the trap on the CS_2 molecules becomes so shallow that it cannot trap the electrons, and no minima are observed in the Ps yield. It seems as if the electron-trapping ability of the acceptors depends on the V_o of the solvent.

In addition, effects were found which could naturally be ascribed to the influence of solvation on the particles, (e. g. pyrrolidine and TEA in n-heptane). These results are fairly strong arguments in favour of the spur reaction model, but they do not, of course, prove unambiguously that the model is correct.

Proposals can be made for new radiation chemistry experiments to test the interpretation of the results. The mobility of the excess electrons in carbon disulphide- n-hexane mixtures will probably show a well-defined minimum (perhaps a factor of about 10 below the hexane value) at the concentration where the lowest Ps formation is measured. The mobilities for these mixtures will be very interesting in view of the difficulties of explaining the fairly large difference between the excess electron mobilities for pure substances. Also measurements of the electron rate constant and of the absorption spectra of CS_2^- (or perhaps $C_2S_4^-$) in the carbon disulphide-n-hexane mixtures would be useful. The intensity of the absorbtion band will perhaps decrease and broaden when further tunelling sets in at higher carbon disulphide concentrations. The results for the other three mixtures can, of course, also be usefully correlated to future experiments (e. g. proton scavenging and solvation time measurements, studies of clustering, etc.).

For the reactions between electron acceptors and Ps, the results show (in accordance with other papers) that o-Ps reacts with the majority of the electron acceptors. This reaction decreases the o-Ps lifetime. The addition of electron donors to the solvent resulting in the formation of CT complexes lowers the reactivity of the electron acceptors, seen as an increases in the o-Ps lifetime. The lowered reactivity of the acceptors in the complex was used to obtain the complexity constant for some CT complexes. This new method for determination of complesity constants may be of importance, especially for systems where the optical method is not applicable as, for instance, in opaque media.

Some of the acceptors were found to inhibit Ps formation. The addition of electron donors with the formation of CT complexes increased the inhibiting effect. The results were interpreted in the framework of the spur reaction model of Ps formation. According to this model the Ps yield depends on the electron-accepting capacity of the electron acceptors in the liquids. This capacity is not solely dependent on the EA of the acceptor but seems more to depend on the "surroundings" of the acceptor. Acceptors which can attach thermal electrons in the gas phase, by breaking bonds or distributing the energy on its vibrational degrees of freedom, will also inhibit Ps

formation. Small acceptors, which cannot attach low energy electrons in the gas phase at low pressure ($\leq 10^{-5}$ mm Hg), can only to a limited extent attach electrons within the ps region in nonpolar solvent without donor properties. Accordingly, the inhibition cross section for Ps formation will be low. If, however, the same acceptors in the nonpolar solvents participate in a CT complex, or if they are dissolved in a solvent with donor properties, the electron-accepting capacity increases because the released energy can then be removed by breaking the weak bond. Under such circumstances the acceptors will consequently inhibit Ps formation.

It would be very interesting to test this interpretation by a direct pulse radiolysis study of the scavenging of electrons by acceptors and CT complexes, in particular in the ps region where formation of Ps takes place. Also the effect of a strongly enhanced electron capture by acceptors taking part in a CT complex in vacuum, as was found by negative ion mass spectroscopy, should be studied further. Some of these investigations are currently being carried out at our laboratory.

Altogether, the results demonstrate that Ps formation in binary mixtures of organic liquids and liquids containing electron acceptors and/or CT-complexes is an interesting topic for further studies. The interpretation of the results indicates that fairly complicated spur processes, which have been only little studied in radiation chemistry, strongly influence the amount of Ps atoms formed. Positronium formation experiments, which are normally faster and easier to perform than typical radiation chemistry experiments, can therefore be used with advantage in the study of some important problems in radiation chemistry.

ACKNOWLEDGEMENT

The work presented in this report was carried out in partial fulfilment of the requirements for obtaining the degree of lic. scient. (Ph. D.). The work was carried out at the Chemistry Department of the Danish Atomic Energy Commission Research Establishment Risø, under the supervision of civ. ing. mag. scient. B. Skytte Jensen and lic. tech. O. E. Mogensen, from July 1972 to December 1975 (with a six-month interruption from February to August 1975).

The author wishes to thank B. Skytte Jensen for his continuous support and interest in the work, and for numerous fruitful discussions concerning chemistry, liquid phase structure and CT-complexes.

He is also indebted to O. E. Mogensen, who formulated the spur reaction model, and whose large knowledge of positrons, Ps and radiation chemistry coupled with his constant interest were of invaluable help for the present work. O. E. Mogensen was the original author of parts of the two articles used in this report.

M. Eldrup also contributed greatly to the author's understanding of PAT and did half the work of formulating the kinetic equations for the bubble shrinkage model.

P. Simonsen, B. Hickel, V. Shantarovich and R. A. Holroyd likewise contributed to the paper and thanks are due to them for making unpublished data available to the author, who is further grateful to E. Larsen for fruitful discussions on negative ion mass spectroscopy and for recording the negative ion mass spectra. Finally the author wishes to express his appreciation of the valuable technical assistance given by N. J. Pedersen and S. Thyssing, and to thank all those at Risø who have assisted him in his daily activities and in producing this report.

REFERENCES

1) P. Jansen, M. Eldrup, O. E. Mogensen and P. Pagsberg, Chem. Phys. 6, (1974) 265-71.

2) P. Jansen, M. Eldrup, B. Skytte Jensen and O. E. Mogensen, Chem. Phys. 10, (1975) 303-312.

3) V. I. Goldanskii, Atomic Energy Review 6, No. 1 (1968) 3-148.

4) V. I. Goldanskii and V. G. Firsov, Annu. Rev. Phys. Chem. 22, (1971) 209-258.

5) V. I. Goldanskii and V. P. Shantarovich, Appl. Phys. 3, (1974) 335-351.

6) R. N. West, Adv. Phys. 22, (1973) 263-384.

7) Positron Annihilation. Proceedings of the Conference Held at Wayne State University on July 27-29, 1965. Edited by A. T. Stewart and L. Roellig (Academic Press, New York, 1967) 438 pp.

8) H. J. Ache, Angew. Chem. 84, (1972) 234-255.

9) J. A. Merrigan, J. H. Green, and S. J. Tao. In: Physical Methods of Chemistry edited by A. Weissberger and B. W. Rossiter, Vol. I, Part 3D (Wiley, New York, 1972) 501-586.

10) O. E. Mogensen, J. Chem. Phys. 60, (1974) 998-1004.

11) C. D. Anderson, Science, New Series 76, 238 (1932).

12) C. D. Anderson, Phys. Rev. 43, (1933) 491-494.

13) P. A. M. Dirac, Proc. Roy. Soc. A126, (1930) 360-365.

14) O. E. Mogensen, Private communication.

15) A. I. Akhiezer and V. B. Berestetskii, Quantum Electrodynamics, (Wiley, New York, 1965) 868 pp.

16) M. Eldrup, Risø Report No. 254 (1971) 115 pp.

17) O. E. Mogensen, (Lyngby, Denmark, 1968, Thesis) 139 s.

18) P. Kirkegaard and M. Eldrup, Computer Phys. Commun. 3, (1972) 240-250.

19) P. Kirkegaard and M. Eldrup, Computer Phys. Commun. 7, (1974) 401-405.

20) P. Kirkegaard, O. Mogensen, Risø-M-1615 (1973) 25 pp.

21) J. D. McGervey. In: Positron Annihilation Proceedings of the Conference Held at Wayne State University on July 27-29, 1965. Edited by A. T. Steward and L. O. Roelling (Academic Press, New York, 1967) 143-154.

22) R. A. Ferrell, Phys. Rev. 108, (1957) 167-168.

23) L. O. Roelling in Positron Annihilation edited by A. T. Stewart and L. O. Roelling (Academic Press, New York, 1967) 127-141.

24) W. T. Sommer, Phys. Rev. Letters 12, (1964) 271-273.

25) C. G. Kuper, Phys. Rev. 122, (1961) 1007-1011.

26) A. P. Buchikhin, V. I. Goldanskii, V. P. Shantarovich, Dokl. Akad. Nauk. SSSR 212, (1973) 1356-1359.

27) B. Levay and P. Hautojärvi, Radiochem. Radioanal. Letters 10, (1972) 309-314.

28) B. Levay, A. Vertes, and P. Hautojärvi, J. Phys. Chem. 77, (1973) 2229-2233.

29) S. J. Tao, J. Chem. Phys. 56, (1972) 5499-5510.

30) E. J. Hart and M. Anbar, The Hydrated Electron, (Wiley, New York, 1970) 267 pp.

31) A. Ore, Univ. i Bergen Årbok, Naturvitenskap Rekke, Nr. 9 (1949) 1-16.

32) S.J. Tao and J.H. Green, J. Chem. Soc. (A), (1968) 408-417.

33) L.J. Bartal, J.B. Nicholas, and H.J. Ache, J. Phys. Chem. 76, (1972) 1124-1129.

34) L.J. Bartal and H.J. Ache, Radiochimica Acta 17, (1972) 205-208.

35) J.B. Nicholas, R.E. Wild, L.J. Bartal, and H.J. Ache, J. Phys. Chem. 77, (1973) 178-182.

36) L.J. Bartal and H.J. Ache, J. Phys. Chem. 77, (1973) 2060-2066.

37) M. Eldrup, V.P. Shantarovich, and O.E. Mogensen, Chem. Phys. 11, (1975) 129-142.

38) R.E. Green and R.E. Bell, Can. J. Phys. 35, (1957) 398-409.

39) R. Foster, Organic Charge-Transfer Complexes (Academic Press, London, 1970) 470 pp.

40) Spectroscopy and Structure of Molecular Complexes edited by J. Yarwood (Plenum Press, London, 1973) 594 pp.

41) Molecular Association, Vol. I. Edited by R. Foster (Academic Press, London, 1975) 365 pp.

42) R.S. Mulliken, J. Phys. Chem. 56, (1952) 801-822.

43) R.L. Flurry, Theoret. Chim. Acta (Berl.) 23, (1971) 1-11.

44) S.P. McGlynn, Chem. Rev. 58, (1958) 1113-1156.

45) J.N. Murrell, Quart. Rev. (London) 15, (1961) 191-206.

46) R.S. Mulliken, J. Am. Chem. Soc. 74, (1952) 811-824.

47) E.L. Chaney, L.G. Christophorou, P.M. Collins and J.G. Carter, J. Chem. Phys. 52, (1970) 4413-4417.

48) S.J. Tao, J. Chem. Phys. 52, (1970) 752-757.

49) R.A. Holroyd and R.L. Russel, J. Phys. Chem. 78, (1974) 2128-35.

50) R.A. Holroyd, Private Communication.

51) R.A. Holroyd and M. Allen, J. Chem. Phys. 54 (12), (1971) 5014-5021.

52) K. Kraus, W. Müller-Duysing, and H. Neuert, Z. Naturforsch. 16a, (1961) 1385-1387.

53) S.D. Christian and J. Grundness, Nature 214, (1967) 1111-1112.

54) V.I. Goldanskii, I.B. Kevdina, V.P. Shantorovich and K. Petersen, Dokl. Phys. Chem. 202, (1972) 268-270.

55) R.J. Celotta, R.A. Bennett and J.L. Hall, J. Chem. Phys. 60, (1974) 1740-1745.

56) M.W. Siegel, R.J. Celotta, J.L. Hall, J. Levine and R.A. Bennett, Phys. Rev. A6, (1972) 607-631.

57) P. Ausloos, Prog. Reaction Kinetics 5, (1970) 113-179.

58) T. Miyazaki and S. Shida, Bull. Chem. Soc. Jap. 38, (1965) 2114-2118.

59) V.L. Tal'Rose and E.L. Frankevitch, J. Am. Chem. Soc. 80, (1958) 2344-45.

60) G. Briegleb, Z. f. Electrochem. 53, (1949) 350-361.

61) E.E. Tucker, S.B. Farnham, and S.D. Christian, J. Phys. Chem. 73, (1969) 3820-3829.

62) T.J. Kemp, G.A. Salmon, and P. Wardman. In: Pulse Radiolysis Proceedings of the International Symposium held at Manchester, April 1965. Edited by M. Ebert, J.P. Keene, A.J. Swallow, and J.H. Baxendale (Academic Press, London, 1965) p. 247-257.

63) G. Beck and J.K. Thomas, J. Chem. Phys. 57, (1972) 3649-3654.

64) J.R. Brandon and R.F. Firestone, J. Phys. Chem. 78, (1974) 792-796.

65) P.M. Rentzepis, R.P. Jones, and J. Jortner, Chem. Phys. Lett. 15, (1972) 480-482.

66) L. Gilles, J.E. Aldrich, and J.W. Hunt, Nature (London) Phys. Sci. 243, (1973) 70-72.

67) V.M. Byakov, V.I. Goldanskii, and V.P. Shantarovich, Dokl. Akad. Nauk SSSR (Ser. Fiz. Khim.), in press. Doklady Physical Chemistry, Proceedings of the Academy of Sciences of the USSR Physical Chemistry Section.

68) R.K. Wolff, J.E. Aldrich, T.L. Penner, and J.W. Hunt, J. Phys. Chem. 79, (1975) 210-219.

69) C.P. Jonah, J.R. Miller, E.J. Hart, and M.S. Matheson, J. Phys. Chem. 79, (1975) 2705-2711.

70) P. Simonsen et al., to be published.

71) V.I. Goldanskii, O.V. Koldaeva, and V.P. Shantarovich, High Energy Chemistry 9, (1975) 55-70.

72) Lj. Josimovic and J. Draganić, Int. J. Radia. Phys. Chem. 5, (1973) 505-512.

73) V. P. Shantarovich, V. I. Goldanskii, Preceedings from Second International Positron Annihilation Conference, Kingston, Ontario, Canada (1971) p. 5.1. Unpublished.

74) R. E. Goans and L. G. Christophorou, J. Chem. Phys. 63 No. 7, (1975) 2821-2829.

75) A. Hadjiantoniou, L. G. Christophorou, and J. G. Carter, J. Chem. Soc., Faraday Trans. II, 69, (1973) 1704-1712.

76) R. P. Blaunstein and L. G. Christophorou, Radiation Res. Rev. 3, (1971) 69-118.

77) L. G. Christophorou, Atomic and Molecular Radiation Physics (Wiley-Interscience, London 1971) 672 pp.

78) J. G. Dillard, Chem. Rev. 73, (1973) 589-643.

79) K. A. G. McNeil and J. C. J. Thynne, J. Phys. Chem. 73, (1969) 2960-2964.

80) R. E. Goans and L. G. Christophorou, J. Chem. Phys. 60, (1974) 1036-1045

81) J. Rademacher, L. G. Christophorou and R. P. Blaunstein, J. Chem. Soc., Faraday Trans. II, 71, (1975) 1212-1226.

82) L. G. Christophorou, A. Hadjiantoniou, and J. G. Carter, J. Chem. Soc., Faraday Trans. II, 69, (1973) 1713-1722.

83) A. Hadjiantoniou, L. G. Christophorou, and J. G. Carter, J. Chem. Soc., Faraday Trans. II, 69, (1973) 1691-1703.

84) B. Hickel, Centre d'Etudes Nucleaires de Saclay, Private Communication.

85) B. Levay and P. Hautojärvi, J. Phys. Chem. 76, (1972) 1951-1956.

86) A. Allen and R. A. Holroyd, J. Phys. Chem. 78, (1974) 796-803.

87) G. Beck and J. K. Thomas, J. Chem. Phys. 60, (1974) 1705-1706.

88) G. Beck and J. K. Thomas, J. Chem. Phys. 57, (1972) 3649-3654.

89) A. Allen, T. E. Gangwer, and R. A. Holroyd, J. Phys. Chem. 79, (1975) 25-31.

90) P. Kirkegaard, Risø-M-1279 (1970) 57 pp.

APPENDIX 1

This appendix gives a short description of the computer program used to obtain the complexity constant for some CT-complexes.

The program calculates the complexity constant (K) of a CT-complex, the extinction coefficient (ε) of the CT-complex, and the extinction coefficient (ε_o) of either the pure donor or the pure acceptor.

The input data can be obtained from a set of measurements of the absorbances (abs) in a CT-band.

The CT-complex must be in a solvent.

The absorbances must be measured for different CT-complex concentrations all at the same wavelength.

For all the measurements, the concentration of the donot $[D_o]$ must be a constant (k) times the concentration of the acceptor $[A_o]$.

The following mathematical models are used:

$$[D_o] = k[A_o]. \qquad (A1.1)$$

Assuming the donor absorbes at the wavelength, the absorbance is (1 cm cell):

$$abs = \varepsilon [AD] + \varepsilon_o(k[A_o] - [AD]) = (\varepsilon - \varepsilon_o)[AD] + \varepsilon_o k[A_o], \qquad (A1.2)$$

where $[AD]$ is the concentration of the CT-complex. Assuming that only 1:1 complexes occur, the complexity constant is

$$K = \frac{[AD]}{([A_o] - [AD])(k[A_o] - [AD])} . \qquad (A1.3)$$

Setting $[A_o] = C$ *and solving (A1.3) for* $[AD]$ *yields,*

$$[AD] = \frac{1}{2}((1+k)C + K^{-1} - \sqrt{(((1-k)C + K^{-1})^2 + 4kC/K)} . \qquad (A1.4)$$

Introducing the substitution

$$\alpha = \varepsilon - \varepsilon_o$$

$$\beta = k(\varepsilon + \varepsilon_o)/2$$

$$x = \frac{C}{2} + \frac{1}{2K} - \sqrt{(0.25((1-k)C + K^{-1})^2 + kC/K)}$$

the absorbance (A1.2) is

$$abs = \alpha x + \beta C$$

now the absorbance is expressed in ε, ε_0, K, k and C.

Using a least squares fitting, the theoretical spectra (A1.2) are fitted to the measured absorbances (Y) in such a way that

$$S^2 = \sum_j (Y_j - \alpha x_j - \beta C_j)^2 w_j \qquad \text{(A1.5)}$$

is minimized. Here j is the index for the different measurements in the series and w is the weight factor given to the individually measured absorbances.

For this problem the unknown α and β (or ε, ε_0) are linear fitting parameters and K is a nonlinear fitting parameter. This means that having a given K, α and β can be calculated directly by setting

$$\frac{dS^2}{d\alpha} = \frac{dS^2}{d\beta} = 0 \qquad \text{(A1.6)}$$

and solving the equations (A1.6) for α and β. This yields

$$\alpha = \frac{\sum_j w_j x_j Y_j \cdot \sum_j w_j C_j^2 - \sum_j w_j Y_j C_j \cdot \sum_j w_j x_j C_j}{\sum_j w_j x_j^2 \cdot \sum_j w_j C_j^2 - \left(\sum_j w_j x_j C_j\right)^2} \qquad \text{(A1.7)}$$

$$\beta = \frac{\sum_j w_j Y_j C_j - \alpha \sum_j w_j x_j C_j}{\sum_j w_j C_j^2} \; .$$

The minimum of S^2 is obtained using Newton iteration method for K

$$K_{n+1} = K_n - \frac{dS^2}{dK} \Big/ \left| \frac{d^2 S^2}{dK^2} \right| \; . \qquad \text{(A1.8)}$$

Recalling that α, β and x depend on K, all differentiations have to be made through these parameters in calculating $\frac{dS^2}{dK}$ and $\frac{d^2S^2}{dK^2}$.

The iteration has converged when $\frac{dS^2}{dK}$ is below a preset value (often 10^{-30}).

A statistical analysis of the output data is also given. This very closely follows the procedure given by Kierkegaard in ref. 90. The program was tested on several synthetic data with excellent results. Used on experimental data, it gave presumably good results. As a check on the output data, the calculated ε_0 can be compared to the value obtained for the pure compound in the same solvent.

The computing time for a typical calculation (10 different abs) is 0.1-0.01 s on a B 6700 computer.

APPENDIX 2

This appendix describes how the gas phase complexity constant between an electron acceptor and donor may be determined by the PV technique. The complex SO_2-TMA is used as example.

Equimolar amounts of TMA and SO_2 were condensed in an ampoule. The temperature of the mixture was increased to room temperature, at which point transparent crystals appeared.

By letting the vapour over the crystals expand into a known volume V and measuring its pressure P, and thereafter condensing the vapour in an ampoule and determining the weight W of the condensed vapour in the ampoule, the gaseous phase complexity constant of the complex was determined as follows.

The vapour is composed of acceptor molecules, donor molecules and complex molecules. Assuming that only 1:1 complexes occur, the total amount of molecules, n, can be determined as:

$$n = (A_o - AD) + (D_o - AD) + AD = 2A_o - AD = \frac{PV}{RT} \text{ mole} \qquad (A2.1)$$

where AD is the amount of complex and A_o, D_o is the total amount of acceptor and donor molecules irrespective of their existence as free molecules or their participation in a complex AD. Here $A_o = D_o$. From the weight W, A_o is determined

$$A_o = \frac{W}{M_w} \text{ mole}, \qquad (A2.2)$$

where M_w is the molar weight of the complex. Combining (A2.1) and (A2.2) we have:

$$AD = 2A_o - n = \left(2\frac{W}{M_w} - \frac{PV}{RT}\right) \text{ mole}, \qquad (A2.3)$$

and the gas phase complexity constant K can now be calculated by use of (A1.3), (A2.2), and (A2.3).

$$K = \frac{AD \cdot V}{(A_o - AD)^2} M^{-1}.$$

For SO_2-TMA, we obtained P = 3.5 mm Hg, V = 9.488 l, W = 0.1204 g, and M_w = 123.17, giving

$$K \approx 1800\ M^{-1}.$$

The gas phase complexity constant for the SO_2-TMA complex has been determined optically by Christian and Grundness[53] to be 340 M^{-1}. The value of K determined here is rather uncertain since $\frac{dK}{dP}$ in this case is $\simeq$ - 9000 M^{-1} (mm Hg)$^{-1}$. The method can be used on other complexes. For complexes with higher vapour pressure, the accuracy can be improved considerably.

ISBN 87-550-0401-6